Anna Lindner, BSc

Alkali activated material Design: Evaluating the influence of composition on mechanical properties and 3D printability

MASTER'S THESIS

to achieve the university degree of

Master of Science

Master's degree programme:

Geosciences

submitted to

Graz University of Technology

Supervisors

Dr. Florian Mittermayr

Institute of Technology and Testing of Construction Materials

Ass. Prof. Dr. Cyrill Vallazza-Grengg, Institute of Applied Geosciences

Graz, March 2026

EIDESSTATTLICHE ERKLÄRUNG

Ich erkläre an Eides statt, dass ich die vorliegende Arbeit selbstständig verfasst, andere als die angegebenen Quellen/Hilfsmittel nicht benutzt und die den benutzten Quellen wörtlich und inhaltlich entnommenen Stellen als solche kenntlich gemacht habe. Die vorliegende Masterarbeit ist identisch mit dem auf TUGRAZonline hochgeladenen Textdokument.

Darüber hinaus erkläre ich hiermit ausdrücklich, dass die Anwendung von Künstlicher Intelligenz, (Chat GPT von Open AI und Perplexity) ausschließlich zur Stil Verbesserung, Rechtschreibüberprüfung und linguistischen Kontrolle verwendet wurden. Zu keinem Zeitpunkt wurden diese Anwendungen angewendet, um wissenschaftliche Inhalte dieser Arbeit zu verändern, zu erstellen oder zu entwickeln.

STATUTORY DECLARATION

I declare that I have written this thesis independently, that I have not used any sources/resources other than those indicated, and that I have explicitly marked all passages quoted verbatim or in substance from the sources used. This master's thesis is identical to the text document uploaded to TUGRAZonline.

Furthermore, I explicitly declare that artificial intelligence applications (ChatGPT from OpenAI and Perplexity) were used exclusively for stylistic improvements, spell checking, or linguistic revisions. At no point were these tools used to create, develop or modify the academic content of this thesis.

…… ……

date (signature)

Acknowledgement

Deep gratitude to everyone at the Institute of Technology and Testing of Construction Materials and the Institute of Applied Geosciences at TU Graz as well as Uni Graz, with whom I have been working over the last years and who also supported me during my studies and with my thesis. In particular, I would like to thank Ognjen Rudic, Gregor Koller, Jürgen Liederer, Rudolf Panik, Marco Riepl, Katharina Weisser, Florian Steindl, Monika Butacevic, Yunus Seyrek, Kevin Milisits, Markus Untersteiner and Dorothee Hippler. I would like to express my gratitude for the valuable support, the team from the 3D- Printing Concrete Laboratory: Alexander Drums, Andreas Trummer, Georg Hansemann, as well the 3D-Printing team of the Architecture Institute of TU Graz, Britta Nader, Milena Stavric, Jauk Julian, Cornelia Ott who helped me with the laboratory work, had an open ear for my questions and inspired me with new approaches and ideas. Special thanks go to Ognjen Rudic for his endless patience and energetic support in especially in the beginning of Master thesis. Not only did he motivate me and explain procedures until I understood everything, but also actively supported me during my laboratory work. When things didn't go as planned, he was there to help. Big thanks go out to Gregor Koller who spared time for helping me, even though he was loaded with work himself, and Monika Butacevic, who helped me to plan the work in the laboratory. As well as Isabel Galan Garcia and Marlene Sakoparnig-Umdasch for guidance on how to write better and what is important in scientific writing - their excellent supervising of my Bachelor thesis spared me a lot of work in this thesis. I would also like to thank Arthur Borzi for taking the time to read through my thesis and for his valuable suggestions and comments. I truly appreciate the effort and thoughtful feedback he provided. Furthermore, I would like to express my sincere gratitude to my supervisors, Florian Mittermayr and Cyrill Vallazza-Grengg, for their precious support throughout this Master thesis. Their productive discussions, numerous ideas and evaluation were instrumental for the finalisation of this thesis. Finally, I would also like to thank my family and friends, who have always supported me and stood by my side no matter what. Words cannot express how grateful I am for everyone’s help. Thank you so much.

Kurzfassung

Durch die Herstellung von herkömmlichem Portlandzement-Klinker werden weltweit hohe CO_2- Emissionen verursacht. Auf der Suche nach umweltfreundlichen Baumaterialien stellt die Verwendung von alkalisch aktivierten Materialien (AAMs) eine vielversprechende Alternative dar. Diese Masterarbeit untersucht die Materialentwicklung von Hüttensand (GBFS) und Metakaolin (MK)- basierten AAMs für 3D-Druckanwendungen. Zudem beschäftigt sich diese Masterarbeit mit der möglichen Verwendung von Spritzbetonbeschleuniger (ACC) in alkalisch aktivierten Systemen. Dazu wurde die Zusammensetzung von Metakaolin, Hüttensand und K-Wasserglas als Aktivator plus weiteren Additiven und Öl sowie Spritzbeton Beschleuniger auf Basis von Na-Aluminat systematisch variiert. Zu den getesteten Parametern zählen rheologische Eigenschaften (Mini-Slump-Test, Fließverhalten), mechanische Eigenschaften (Zug- und Druckfestigkeit), Abbindezeit Pumpbarkeit und Druckbarkeit. Die Ergebnisse zeigen, dass die Wahl der Materialien einen signifikanten Einfluss auf den Abbindeprozess und damit auf die Verarbeitbarkeit und Druckbarkeit hat. Zudem wiesen in dieser Studie entwickelte Mischungen höhere Druckfestigkeiten (>52 N/mm² nach 7 Tagen Aushärtezeit) als für den 3D-Druck verwendetes Referenzmaterial (Baumit PrintCret 230), auf. Die Ergebnisse der Wärmeentwicklungsmessungen sowie der Abbindezeit zeigen, dass die Verwendung einer Beschleunigerdosierung von 3 % kürzere Abbindezeiten und eine beschleunigte Frühfestigkeitsentwicklung ermöglicht. Der 3D-Druck der entwickelten Mischungen wurde erfolgreich getestet und zeigte, dass die Optimierung der Fließfähigkeit und Viskosität entscheidend für die Druckqualität ist. Diese Arbeit stellt Zusammenhänge zwischen Reaktionsverhalten, Materialperformance und Zusammensetzung her. Dies induziert, dass optimierte Zusammensetzungen nicht nur die Festigkeit erhöhen, sondern auch Möglichkeiten bieten, die Eigenschaften für bestimmte Anforderungen anzupassen. Diese Studie liefert neue Erkenntnisse zur Entwicklung nachhaltiger Baumaterialien und unterstreicht das Potenzial von schlackenbasierten AAMs für nachhaltige Anwendungen in der Bauindustrie.

Abstract

Compared to the production of conventional Portland cement clinker, which is responsible for a significant share of global anthropogenic CO_2 emissions, the use of alkali-activated materials (AAMs) offers a potentially lower-carbon binder alternative. This Master's thesis investigates the use of granulated blast furnace slag (GBFS) and Metakaolin (MK) based AAMs for 3D printing applications. A systematic variation of mixture composition including metakaolin, GBFS various additives, oil, as well as varying dosages of shotcrete accelerator was investigated, to optimise rheology, mechanical performance, pumpability and printability. Parameters tested included rheological properties (mini-slump test, flow behaviour), mechanical properties (tensile and compressive strength), setting time, pumpability and printability. The basic concept is illustrated in the Graphical abstract below. The GBFS/MK based AAMs developed in this thesis showed a compressive strength of >52 N/mm² after 7 days and exceeded a commercial reference material (Baumit PrintCret 230). The results from heat development measurements as well as the setting time, indicate that the use of an ACC dosage of 3% enables shorter setting times and increases reaction rate. The 3D printing of the developed mixtures was successfully tested, showing that a balance between flowability and viscosity is critical for print quality. Furthermore, results show that the choice of raw materials and additives has a significant effect on the reaction kinetics and structural build-up and consequently on processability. This suggests that optimised compositions not only increase strength but also enable tailoring of material properties for specific construction applications. These findings indicate that properly designed, slag-based AAMs can achieve rapid strength development and suitable fresh state behaviour for additive manufacturing. This study establishes relationships between composition, reaction behaviour and performance to provide new insights into the development of sustainable building materials and highlights the potential of AAMs for applications in the construction industry.

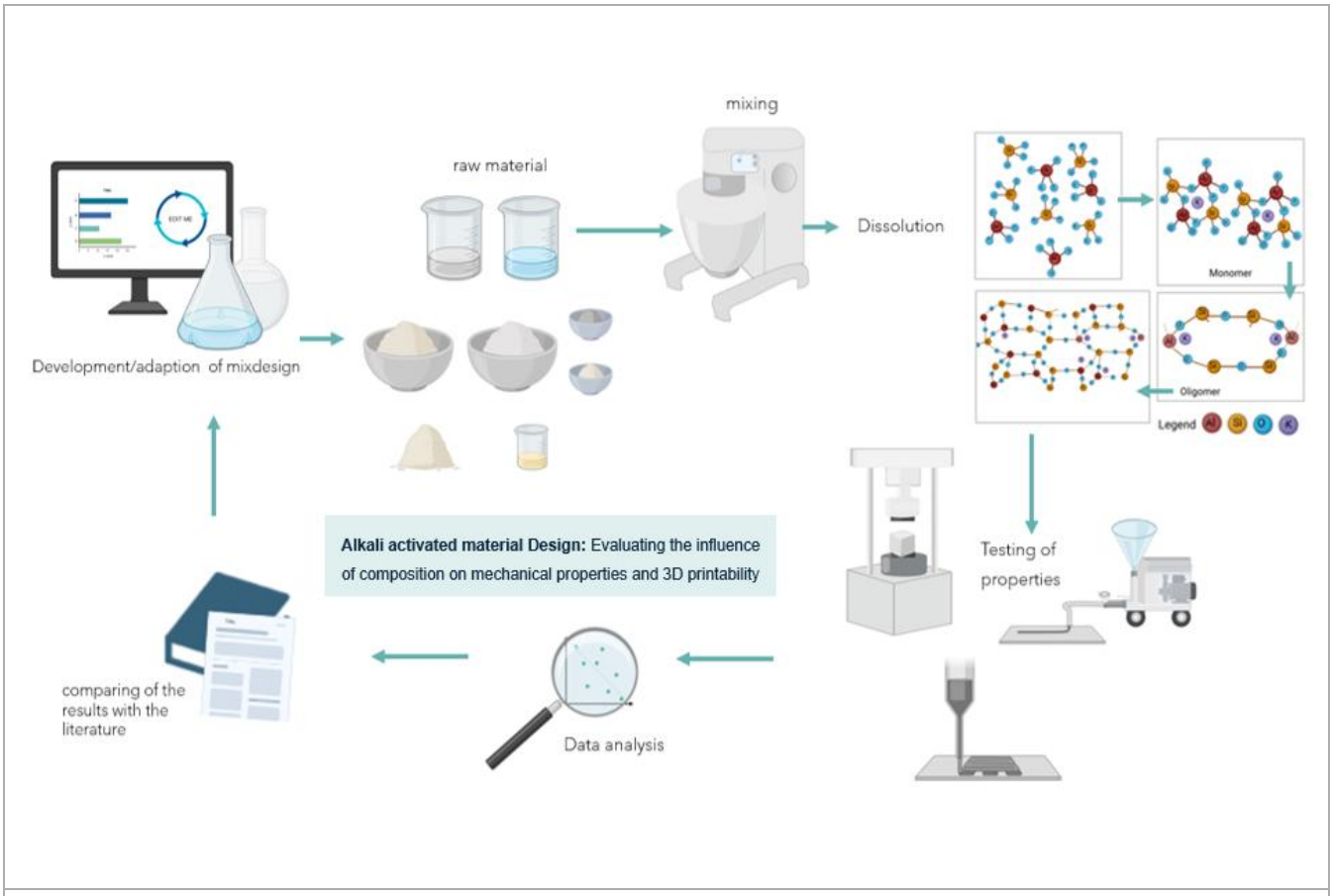

Graphical abstract showing the basic concept of the master thesis (created with BioRender)

TABLE OF CONTENTS

Abbreviations

3D	three-dimensional
AAM	alkali-activated material
AAS	alkali activated slag
ACC	accelerator
AM	additive manufacturing
C&D	construction and demolition
C-(N)-A-S-H	Calcium Sodium Aluminosilicate Hydrate Gel
C-A-S-H	Calcium Aluminosilicate Hydrate Gel
GBFS	granulated blast furnace slag
GP	geopolymer
HPC	high performance Calorimeter
IC	Isothermal conduction Calorimeter
l	liters
MK	Metakaolin
ml	milliliters
M_O, M_R	metakaolin-Types O und R
N-A-S-H	Sodium Aluminosilicate Hydrate Gel
OPC	ordinary Portland cement
REF	reference mixture
RH	relative humidity
SWS	steelworks slag
W/SRM	waste- and secondary raw material
WG	waterglass
WG 1.7	waterglass with a molar ratio of K_2O/SiO_2 1.7

Glossar

activator	Alkaline material in liquid or solid form such as sodium or potassium hydroxides and silicates
alkali activation	chemical process in which aluminosilicate materials react with alkaline activators to form binding phases
L/d	aspect ratio, length-to-diameter ratio of fibres
precursor	Fine powder materials with high content of aluminosilicate and/ or calcium e.g. metakaolin, blast furnace slag, coal fly ash
w/s	water-to-solid ratio

1 RESEARCH QUESTION AND GOALS

The main goal of this thesis is to investigate and optimize the properties of alkali-activated materials (AAMs), focusing on the influence of composition on mechanical properties and suitability for 3D printing. To achieve that, existing recipes were adapted and new ones developed. In addition, these recipes were optimized according to their determination in rheological properties, print and pumpability, as well as strength development. This thesis aims to answer the subsequent questions:

- How can GBFS/MK-based AAM formulations be designed and optimised to meet the specific requirements of 3D printing, particularly in terms of printability and mechanical performance?

- Which compositional parameters (e.g. binder composition, activator chemistry, and additive dosage) govern the rheological behaviour and setting kinetics of AAMs relevant to additive manufacturing?

- What factors influence the interlayer bonding and structural integrity in 3D-printed AAM elements?

- How does the chemical modification (mix design, additives such as oil, etc.) of the mixture design and processing parameters affect the workability and fresh-state stability of AAMs?

- Are shotcrete accelerators suitable for the use in 3D printed AAMs, and how do they influence reaction kinetics, setting behaviour and mechanical performance?

2 INTRODUCTION

2.1 Background and Motivation

The growing world population and the associated high demand for infrastructure development leads to increasing consumption of construction materials, particularly ordinary Portland cement (OPC). Since the production of OPC requires energy-intensive processes such as clinker firing and raw material calcination, it generates large amounts of CO_2 emissions, accounting for approximately 8 % of total CO_2 emissions worldwide [1], [2]. In addition to CO_2 emissions, construction and industrial waste are a growing problem. Despite recycling efforts, a large proportion still ends up in landfills. According to [3], construction and demolition (C&D) activities account for approximately 38 % of all waste generated in the EU, corresponding to around 845 million tonnes per year. A significant fraction of this consists of mineral-based materials such as concrete, bricks, and ceramics, with concrete alone estimated to generate more than 50 % of total C&D waste [3]. Consequently, the cement industry is under rising pressure to improve its carbon footprint, which makes the search for OPC alternatives and research in this area a priority [4], [5]. The Euroslag/ FEhS assessment for 2023 indicates a total of 35.8 million tonnes of steel slag for the EU + UK, including 19.9 million tonnes of blast furnace slag (BFS) and 15.9 million tonnes of steelworks slag (SWS)[6]. The use of such industrial by-products in cement production prevented the extraction of 44 million tonnes of natural rock across Europe in 2022 and avoided approximately 12 million tonnes of CO_2 emissions [6]. These amounts highlight the urgent need for sustainable solutions and circular approaches in the construction sector, particularly through the reuse and valorisation of mineral residues and the replacement of CO_2-intensive materials such as OPC.

2.2 Alkali-Activated Materials and Geopolymers

Among the emerging alternatives, alkali-activated materials (AAMs) have attracted considerable attention due to their ability to utilise industrial by-products and mineral waste streams as precursors [7]. AAMs comprise a broad class of binders produced through the alkaline activation of aluminosilicate precursors with high amounts of (Al) alumina and (Si) silicon, such as fly ash, metakaolin, or granulated blast furnace slag (GBFS) [7]. Those precursors combined with an alkaline activator, which consists of alkali metal silicates and/or alkali metal hydroxides [8] [9], depending on the Ca- content of the AAMs different gels are

formed. Low Ca-content referring to the term *geopolymer* (GP) usually based on fly ash or metakaolin, in which the binding phase is a sodium or potassium aluminosilicate gel (N/K–A–S–H) that forms a three-dimensional polymer network of Si–O–Al, with SiO_4 and AlO_4 tetrahedra, cross-linked by oxygen bridges. The gaps in these networks are filled by alkaline cations (K^+, Ca^{2+}, Na^+, and H_3O^+), which counteract the negative charge of Al^{3+}. With higher amounts of Ca content and corresponding production of a Ca-bearing aluminosilicate hydrate gel are more likely to form in the alkaline activation process (C-A-S-H) than Al and alkalis (Na and/or K) [7]. Because of the significant contribution of Ca- bearing hydrate phases, the materials investigated in this study are more accurately described as MK-GBFS-based AAMs or Hybrid-AAM (GBFS + Metakaolin, K_2SiO_3-activated), rather than conventional geopolymers. These systems combine the reactivity and strength potential of slag with the environmental benefits of geopolymer chemistry, making them highly promising for innovative applications such as 3D printing [7], [10]. Produced binders exhibit similar mechanical and durability characteristics to OPC-based systems. Numerous research projects focus on the use of MK- alkali activated slag (AAS) based AAMs as sustainable binders, showing advantages such as high strength and chemical resistance but also facing challenges related to processing and reactivity [11], [12].

2.3 Additive Manufacturing in Construction

Additive manufacturing (AM) in construction, particularly 3D concrete printing, carries great potential to revolutionise building processes. By eliminating the need for conventional formwork, 3D-printing concrete may potentially reduce material by 30–60 %, streamline supply chains, and lower the environmental impact of transport and logistics [13]. However, this technology demands customised material properties such as tailored rheology, setting behaviour, and interlayer adhesion [14], [15]. Conventional AAMs as developed for casting applications, often do not meet all required criteria of extrusion-based 3D printing from their intrinsic characteristics. This challenge is intensified by the still limited practical experience and the lack of standardized design guidelines for MK-GBFS based AAMs in 3D printing. Currently, research gaps exist regarding the adaptation and evaluation of MK-GBFS based AAMs specifically for 3D printing applications [7], [11], [16]. However, AAMs exhibit different properties in both their fresh and hardened states, regarding their diverse material composition and complexity. This diversity could be leveraged to tailor AAMs to specific construction techniques, equipment, and operational conditions highlighting their potential to improve traditional construction [16].

3 MATERIALS

In this section, the source materials, of the experimental part of the thesis are described and illustrated in detail. In this thesis different types of aluminosilicate raw materials (precursors) aluminosilicate activators, water, aggregates, and oil were used for paste- and mortar production. A schematic overview of the used materials is visible below in Figure 1.

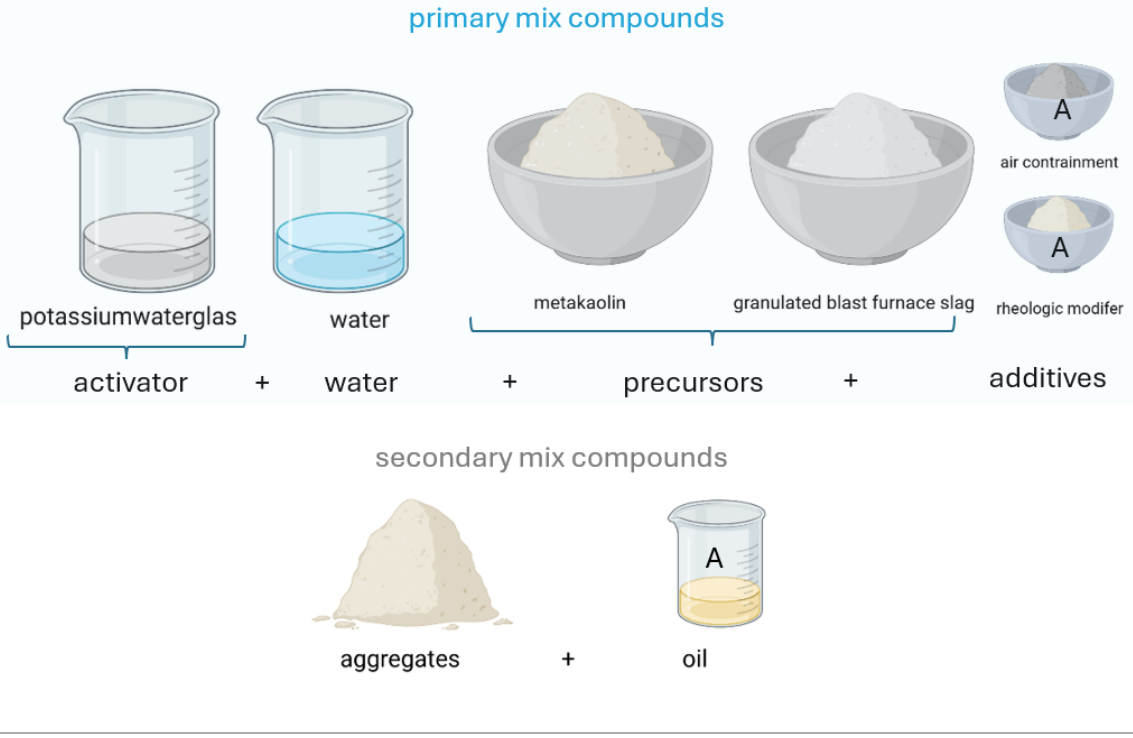

Figure 1 schematic illustration of the ingredients used for the mixtures in their respective mixing order. Additives used to adjust the material properties are marked with (A) (created with biorender)

3.1 Aluminosilicate precursors

Precursors used in this study include materials such as metakaolin, granulated blast furnace slag [17].

Metakaolin

In this thesis two different metakaolin types were used: MetaverO (M_O) [18] and MetaverR (M_R) [18], [19], their chemical composition and physical properties are visible in Table 1.

Table 1 Metakaolin, chemical composition [wt.%] and physical properties

Type	SiO_2	Al_2O_3	Fe_2O_3	K_2O	CaO	MgO	Na_2O	Bulk density	colour	Grain size distribution
M_O	53- 54	41 – 44	< 0.5	< 1.0	n.a.	n.a.	n.a.	2.6 g/cm^3	white	d50 3.2 µm- d90 15 µm
M_R	66-69	26-28	<2.4	<0.2	<0.8	<0.1	<0.1	2.6 g/cm³	reddish	d50 15 µm- d90 40 µm

Granulated blast furnace slag (GBFS)

GBFS is a conventional by-product from steel and iron industry that has latent hydraulic activity and is commonly used as supplementary material in cementitious and AAM systems [20]. The major oxides of GBFS are calcium oxide (CaO), silicon dioxide (SiO_2), magnesium oxide (MgO) and aluminium oxide (Al_2O_3). In smaller quantities GBFS contains approximately less than 10% of the following components: iron oxide (FeO), titanium oxide (TiO_2), sulfid(S^{-2}), sulfat (SO_4^{2-}), manganese oxide (MnO), sodium oxide (Na_2O) as well as potassium oxide (K_2O) [21].

BanahCEM powder

BanahCEM powder[22] was used for the basic mixtures (BR1-BR6, BA1-BA3) based on the mixtures which were previously developed at TU Graz. BanahCEM is a blend of ground granulated blast-furnace slag and metakaolin-rich calcined clay the chemical composition of it is visible in Table 2 [23].

Table 2 BanahCEM powder, chemical composition [wt%]

Type	SiO_2	Al_2O_3	Fe_2O_3	CaO	MgO	MnO	TiO_2	Na_2O	K_2O	SO_3	P_2O_5
BanahCEM powder	32.04	25.99	25.21	7.78	1.71	0.37	3.17	0.36	0.15	0.22	0.14

3.2 Alkaline activator

In this study two different potassium silicate solutions (potassium waterglass) were used as activators, their chemical compositions are summarized in the Table 3. For the basic mixtures a potassium WG (BanahCEM liquid) was used containing a molar ratio of 1.91 SiO/ K_2O For the hybrid mixtures a WG with a molar ratio of 1.7 SiO_2 / K_2O was used.

Table 3 Chemical composition of the used alkaline activators

Type	H_2O [wt.%]	molar ratio SiO_2 /K_2O	mass density [g/cm³]
WG 1.7	55	1.70	1.52
BanahCEM liquid	35	1.91	1.72

3.3 Additives

Rheological modifier

A thixotropic thickening and suspending agent based on attapulgite clay was added to improve the consistency of the mixture and to modify its rheological behaviour. This modifier is called attagel and has a density of 2.40 [g/cm³] [26].

Air entrainment

A reactive air entrainment agent based on calcium carbonate and metal compounds was added to improve the void distribution in the AAM matrix, and thus increase frost-deice salt resistance, resulting in enhanced durability. This air entrainment is called SikaControl® AER-200 P and has a bulk density of 1.30 [g/cm³][27].

3.4 Aggregates

Aggregates are required in mortar production to enhance mechanical stability and improve the bulk properties of the material. Standard sand with a grain size of 0-2 mm and a mass density of 2.65 g/cm³ [28] was used for the mortar production.

3.5 Oil

Following previous work [23], [29] at TU Graz, vegetable oil was added as a pore size modifying agent. The oil, utilized for the mixtures, is a conventional heat-treated (175°C) sunflower seed oil with a mass density of 0.92 kg/m³ [23].

3.6 Accelerators (ACC)

Accelerators are used to shorten the setting time of cementitious materials, like shotcrete or in the 3D printing. In this thesis, experiments with a shotcrete accelerator were conducted to investigate its suitability for 3D printing alkali-activated geopolymers, and its influence on material performance. The used shotcrete accelerators are presented below in Table 4 [30].

Table 4 Shotcrete ACC, Chemical composition [wt.%]

Type	Al_2O_3	Na_2O	solids
SIKA Sigunit®L22	24	19	43

3.7 Reference material

A functioning reference material was used to evaluate the developed material for 3D printing. Measured properties were compared with the reference values to determine the differences in performance. Both cement and accelerator used for the reference material are summarised in Table 5 (manufacturer data Baumit PrintCrete system).

*Table 5 Chemical composition and details of the reference material. *Recommended dosage of added water*

Type	Basis	Density [g/cm³]	Water [%]	Maximum grain size [mm]	Recommended dosage	Tensile strength [N/mm²]	Compressive strength [N/mm²]
PrintCret 230	Grey cement with fillers and additives	~1.99	14–16 *	2	Typically, 1.9–2.0 kg/m³ fresh mortar	6–10	45–55
AdSpeed 200	Aluminium sulfate solution	~1.35–1.45 (liquid)	55–65	0 (fully liquid)	4–8 % of binder weight	–	–

4 MIX DESIGN DEVELOPMENT

This section describes the systematic development of the mix design development in the three stages (section 4.1- 4.3). Different AAM formulations, from initial paste level mixtures to 3D printable mortars were developed.

The initial paste-level mixtures (I1-I3) were prepared to investigate the influence of different precursors, such as metakaolin and granulated blast furnace slag (GBFS), on workability and early strength. Based on previous work at TU Graz, mixtures with a GBFS-to-metakaolin ratio of 3:1 were preselected as the starting point to select potential binder material. The formulations consisted of metakaolin, GBFS, oil, water, and waterglass. All mixtures were prepared using a Vortex mixer, according to the procedure described in section 5.2.1. The mix proportions of the initial paste series (I1-I3) are presented in the Table 6.

Table 6 Mix proportions of initial paste-level development [wt.%]

	Metakaolin		**waterglass**	**GBFS**	**Oil**	**water**	
Mix	**M_O**	**M_R**	**WG 1.7**	**4500**		**H_2O**	**SUM**
I1	52.63	-	34.74	-	2.11	10.53	100
I2	14.23	-	41.28	42.70	1.78	-	100
I3	-	14.55	40.00	43.64	1.82	-	100

4.1 Mortar-level optimization

The optimisation at the mortar level aimed to adjust the rheological behaviour and flow characteristics of the previously developed 3D-printable, alkali activated pastes. Based on literature for 3D-printing applications, slump values of 115–200 mm were aimed [31]. Therefore, the influence of water content, aggregate proportion, and rheological modifiers was systematically investigated. All mortar mixtures (Series 1-3) were prepared using a Hobart mixer according to the procedure described in Section 5.2.3.

Variation of mix parameters

Three series of mortar mixtures were developed:

- **Series 1:** Basic formulation with varying rheological modifier dosage (Table 7: BR1–BR6).

Table 7 Basic formulation mix proportions with varying amounts of rheological modifier [wt.%]

	BR1	BR2	BR3	BR4	BR5	BR6
Potassium waterglass	16.83	16.80	16.79	16.77	16.76	16.69
BanahCEM	24.25	24.22	24.19	24.17	24.15	24.05
Air entrainment (SikaControl® AER-200 P)	0.05	0.05	0.05	0.05	0.05	0.05
Oil	4.95	4.94	4.94	4.93	4.93	4.91
Water	6.09	6.09	6.08	6.07	6.07	6.04
rheological modifier (Attagel)	0.49	0.64	0.74	0.83	0.92	1.35
Aggregate 0/2	47.02	46.95	46.91	46.86	46.82	46.62

- **Series 2:** Basic formulation with varying aggregate content (Table 8: BA1–BA3).

Table 8 Basic formulation with different aggregate contents modified mix proportions [wt.%]

	BA1	BA2	BA3
Potassium waterglass	18.68	16.83	15.31
BanahCEM	26.92	24.25	22.07
Air entrainment (SikaControl® AER-200 P)	0.05	0.05	0.05
Oil	5.49	4.95	4.50
Water	6.76	6.09	5.55
rheological modifier (Attagel)	0.55	0.49	0.45
Aggregate 0/2	41.20	47.02	51.80

- **Series 3:** MK- GBFS based formulations (HM1-HM7)

Table 9 MK- GBFS based mixtures mix proportions [wt.%] ·

	HM1	HM2	HM3	HM4	HM5	HM6	HM7
Potassium waterglass	16.02	16.16	16.59	16.93	17.06	17.56	17.56
GBFS	5.23	13.47	20.74	21.16	21.32	18.74	18.74
M_O	20.51	13.47	6.91	7.05	7.11	6.51	3.25
M_R	0.00	0.00	0.00	0.00	0.00	0.00	3.25
Air entrainment (SikaControl® AER-200 P)	0.07	0.07	0.07	0.07	0.07	0.05	0.05
Oil	3.93	2.15	2.21	2.26	2.27	2.58	2.58
water	5.23	5.28	2.76	0.79	0.00	0.00	0.00
rheological modifier (Attagel)	0.66	0.67	0.69	0.70	0.71	0.52	0.52
Aggregate 0/2	48.07	48.48	49.76	50.78	51.18	49.06	49.06

4.2 Accelerated mixtures

Pastes or mortar

To determine the impact of an acceleration agent, selected mixes were further adjusted by adding different proportions of a shotcrete accelerating agent (SIKA Sigunit®L22) [30] . The selection of the mixes was based on mechanical properties and workability parameters to provide a reasonable overview of the mixes with 3% were chosen and further tested in many tests. Depending on the test method either paste mixtures or mortar mixtures were used. Two mixtures HM4, HM7 were prepared using different dosages of accelerator 0%, 3%, 5%, 7% (ACC). All accelerated mixtures (HM4_0%ACC, HM4_3%ACC, HM4_5%ACC, HM4_7%ACC, HM7, HM7_3%ACC, HM7_5%ACC, HM7_7%ACC) were prepared using an overhead mixer, according to the procedure described in section 5.2.2. The pastes were further tested with different methods see (Figure 5).

5 METHODS

In this section, the conducted experimental procedures used in this thesis are described and illustrated.

5.1 Weighing of the ingredients

Prior to the mixing procedure, the ingredients for each mixture were weighed using a precision scale. The list of ingredients for each mixture is shown in the mix development section. Typical weighed ingredients are shown in Figure 2 and Figure 3.

Figure 2 Ingredients for the mixing procedure of the HM7

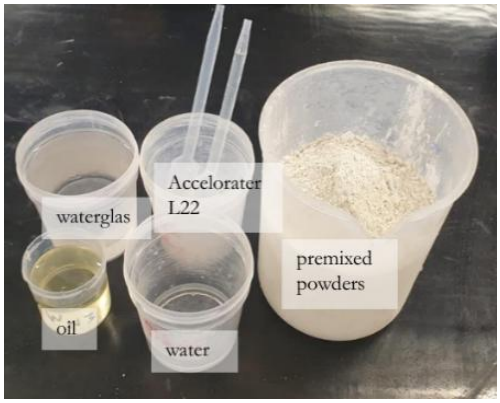

Figure 3 Weighed ingredients for accelerated mixture (HM4_3%ACC)

5.2 Mixing

Depending on the requirements, the type (accelerated mixtures, paste or mortar mixtures) the volume of mixtures and the respective test method, different mixers had to be used. In addition, the capacity and conditions in the respective laboratories also played a role. This section describes which mixer was used for which mixture. The different types of mixers are illustrated in Figure 4.

vortex mixer(created with biorender)	*Overhead mixer*	*Compulsory mixer DIEM Werke*	*Hobart mixer*	*Drill with paddle*

Figure 4 Different mixers used for mixing procedure

5.2.1 Vortex mixer

The vortex mixer (Velp Scientifica ZX4) [32]was used for the preparation of the initial paste-level mixtures (I1-I3) (section 4). For each mixture, 8 samples were produced. All ingredients were weighed prior to mixing (section 5.1). The dry components were placed in a single mixing vessel and manually pre-mixed using a spoon. Subsequently, waterglass and water were added and blended in the vortex mixer at 2400 rpm[32] until a homogeneous consistency was achieved. After mixing for 90 seconds, the workability of I1-I3 (section 5.3.1) was determined. The samples were poured into small cylindrical plastic moulds with approximate dimensions of 30 × 30 mm. The samples were compacted on a vibrating table for 60 seconds to remove entrapped air and sealed immediately with a plastic lid. The specimens were stored at 20 °C and 95 % relative humidity for 1 and 7 days prior to compressive strength testing (see 5.3.2).

5.2.2 Overhead mixer

Preliminary tests revealed that the Vortex mixer was not entirely suitable for paste mixtures containing accelerators (ACC). Thus, an overhead mixer (see figure 7) was used. For each mixture, the powder components were pre-mixed with a spoon and placed under the stirrer. Next the waterglass and water were added. To ensure a homogeneous blending process, the mixing speed was gradually increased to 1000 rpm [33]. After one minute, the mixer was stopped, and the walls of the vessel were scraped down with a spatula to ensure

homogeneous blending. Mixing was then resumed, and after approximately 2.5 minutes, the oil was added to the mixture. The total mixing time was three minutes. Shortly after the ACC was added. During this step, the mixing speed was increased to 1500 rpm to ensure complete dispersion of the accelerator, which had to be mixed rapidly due to its high reactivity. After mixing, the fresh pastes were poured into 3 cm silicon cube moulds with 27 millilitre (ml) volume. The samples were compacted on a vibration table for 60 seconds and stored at 95 % relative humidity and 20 °C.

5.2.3 Hobart mixer

The mixing procedure was carried out using a Hobart mixer with a total volume of 4.5 litres[29]. 15 different mortar formulations were prepared (BR1-BR6, BA1-BA3, HM1-HM7) (see Section 4.1). All ingredients were weighed prior to mixing (section 5.1). The powder components were pre-mixed with a spoon and placed in the mixing bowl below the Hobart mixer. Subsequently, waterglass and water were added, and the mixing was started at low speed. After 30 seconds, the walls of the bowl were scraped down with a spatula to improve the homogeneity of the materials. Mixing was then continued, and the speed was gradually increased according to the standard protocol. After approximately 2.5 minutes of mixing, pre-mixed sand and oil were added to the mixture to ensure a homogeneous consistency. The fresh mixtures were tested to determine rheological behaviour. For the determination of the strength development (see section 5.3.2) the fresh mixtures were cast into prism moulds (40 × 40 × 160 mm³), compacted on a vibrating table for 60 seconds, sealed with a plastic lid and stored at 20 °C and 95 % relative humidity for 1 or 7 days.

Mixing and preparation of ACC and reference mixtures

A total of eight mixtures were prepared to evaluate printability, strength development and setting time of the accelerated systems and the reference system. These included two developed mixtures HM4 and HM7, each produced with and without ACC, as well as four reference mixtures containing different dosages of accelerator (ACC: 0%, 4%, 5.5%, and 7%). The mixing procedure described in section 5.2.3. was applied. The only adjustment was that the accelerator was added shortly after the initial mixing time of 3 minutes. The addition of ACC was performed quickly and followed by intensive mixing at maximum speed (≈ 1500 rpm) for approximately 15 seconds. The fresh mixtures were tested using the Vicat needle (5.3) to determine setting time and a silicone pump to evaluate printability (see section 5.4.2). For the determination of the strength development (see section 5.3.2). The

fresh mixtures were cast into prism moulds (40 × 40 × 160 mm³), compacted on a vibrating table for 60 seconds, sealed with a plastic lid and stored at 20 °C and 95 % relative humidity for 7 and 28 days. The results of the different testing methods are presented in section 6 and compared with the reference material in the discussion.

5.2.4 Compulsory mixer

Methods such as pump tests require larger amounts of material; therefore, a high-capacity compulsory mixer was used for the pumpability trails (Figure 4). Three mixtures, BA1, HM4, and HM7 were prepared, each with a total volume of 6 litres (l). The liquid components were added first; followed by the powder materials. After approximately 2.5 minutes the pre-mixed sand and oil were added and mixing was continued. After mixing, the fresh material was transferred into a funnel and tested for pumpability using the procedure described in Section 5.4.1. Additionally, small amounts of each AAM mixture were cast into prisms (40 × 40 × 160 mm³) and cured for seven days at 95 % relative humidity and 20 °C for subsequent strength testing (see section 5.3.2).

5.2.5 Mixing with a drill

To test the 3D printability of the (HM4, HM7) with a 3D-printer, a drill with attached paddle was used to mix the weighed ingredients. The premixed powder components and the liquid ingredients were added in the bucket and then mixed with the drill. After about 2.5 minutes, the premixed sand and oil were added to the mixture. The mixing continued until the mixture seemed homogeneous. Afterwards, the mixture was filled into a tank to evaluate extrudability and printability (section 5.4.3).

5.3 Methods for characterization of the physiochemical behaviour of the mixtures

In Figure 5 below the experimental test methods for physiochemical behaviour and the corresponding samples for each mixture are summarized and illustrated.

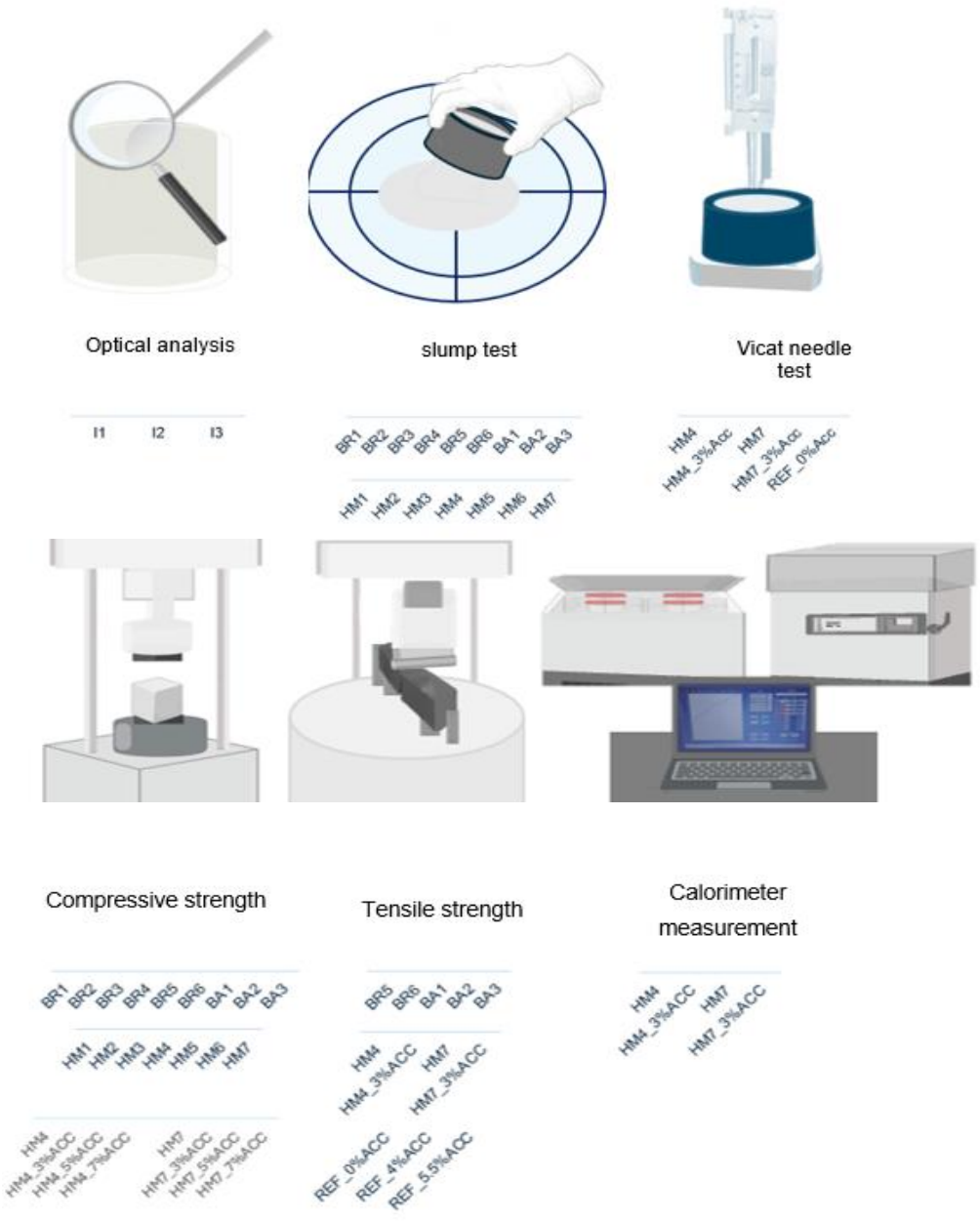

Figure 5 Schematic illustration of experimental test methods for physiochemical behaviour and the corresponding samples for each mixture (created with biorender)

5.3.1 Workability and Rheology

To evaluate the workability and rheological behaviour of the mixtures, the following tests were conducted.

Optical analysis of mixing behaviour and workability

For the initial paste level mixtures(I1-I3) the workability was determined visually.

Slump test

To investigate the mixtures flowability and workability as well as the rheological parameters, a set of slump tests with 16 different recipes have been conducted according to ÖNORM EN 1015-3 [34].

Therefore, different samples were carried out based on the following formulations:

- Basic formulation with varying amounts of rheological modifier (BR1- BR6)
- Basic formulation with different amounts of aggregates (BA1- BA3)
- Hybrid mixtures with basic mixture and GBFS based mixtures (HM1- HM7)

The mixtures (Mortar-level optimization 4.1) were previously mixed with a Hobart mixer (see section 5.2.3) and then filled in a Hägermann cone (Ø 100 mm x 60 mm). After pulling the cone upwards and allowing the material to flow unreservedly, visible in Figure 6, the diameters were measured, using a measuring tape or a vernier caliper, as shown in (Figure 6). To get more insight in the behaviour of the material and gain knowledge about the beginning of the setting time and the initial setting time, a Vicat needle test was conducted.

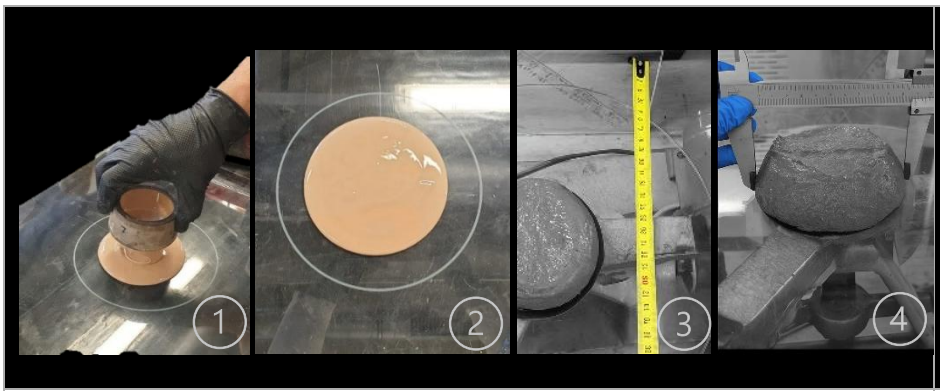

Figure 6 Slump test ÖNORM EN 1015-3: removing of the Hägermann cone (1) and before the measurement (2), Slump test of a mortar mixture before (3) and after the hits (4)

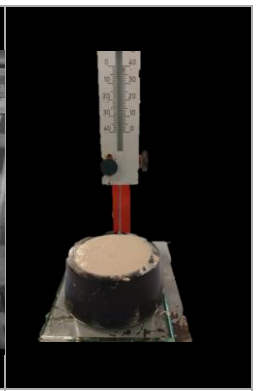

Figure 7 Vicat needle test

Vicat Needle test

To determine the time frame for the workability window for possible printing try-outs in the future, as well as the specific setting behaviours of the mixtures the Vicat needle test (Figure 7) was done on 5 samples (HM4, HM7, HM4_3%ACC, HM7_3%ACC , REF _5.5%ACC) following ÖNORM EN196-3:2016 [34]. The fresh material was filled in the hard rubber Vicat cone, with a diameter of 92 mm and height of 40 mm. Other than in the standard procedure this test was conducted without the storage of the Vicat ring underwater, instead it was performed in dry conditions, also the standard stiffness was not determined.

5.3.2 Strength Development

After the curing of the samples at 95% RH and 20°C for a timespan of either 1 or 7 days the strength development of the mixtures was tested. The results of the strength development are visible in the Chapter 6. The samples with a prism form of (40 x 40 x 160) mm³ were tested following ÖNORM EN – 1015-11 [35] using a hydraulic press from ToniTech.

Tensile strength

The tensile strength was conducted on two prisms per mixture. The tested mixtures are listed in Figure 8. The setup of the tensile strength is visible in Figure 8 the test is conducted until failure, resulting in the sample splitting in two halves.

Compressive strength

With the remaining halves of the prisms from the previously done tensile strength test, the compressive strength was conducted, as shown in Figure 8. Furthermore, accelerated paste mixtures (HM4 and HM7 with different amounts of ACC) were additionally tested for their early strength development which was measured after 3h, 6h and 24 hours.

Figure 8 Compressive strength (left) and tensile strength test (right) of BA1

5.3.3 Reaction kinetics

The heat evolution of the developed paste mixtures was determined using an isothermal conduction calorimeter (I-Cal 4000 HPC) (Figure 9,1-4) [32]. To determine the influence of the accelerator on the reaction kinetics, four samples were prepared: two mixture types (HM4, HM7) containing 0 % and 3 % accelerator (ACC). The pastes were mixed with an overhead mixer (5.2.2) and an amount of 50 g of each fresh sample was placed in in a standard container (~120 ml)[32] for calorimetry(Figure 9, 1). The accelerator was added by mass to the solid binder mass. The start times of the waterglass and accelerator additions were recorded to ensure consistent data collection. The calorimeter was running at 20 °C for 48 h and calibrated before testing. Data were processed using Cal Metrix software(Figure 9, 4). A small portion of each mixture was also cast into prisms for later strength testing (see Strength development). Results are presented in Chapter 6.

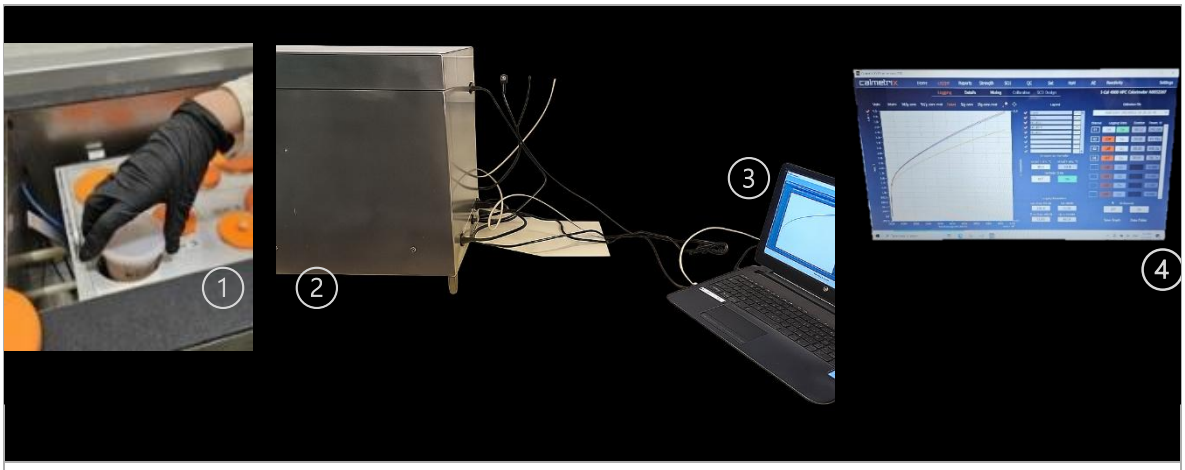

Figure 9 Set-up for the calorimeter measurement: (1) filling one of samples in the channel, (2) The isothermal conduction calorimeter, (3) computer running the calorimeter, (4) Calmetrix program for the analysis

5.4 Methods to test the pumpability and printability for 3D- printing

In the following Figure 10 below illustrates the experimental test methods for pumpability and printability and the corresponding samples for each mixture.

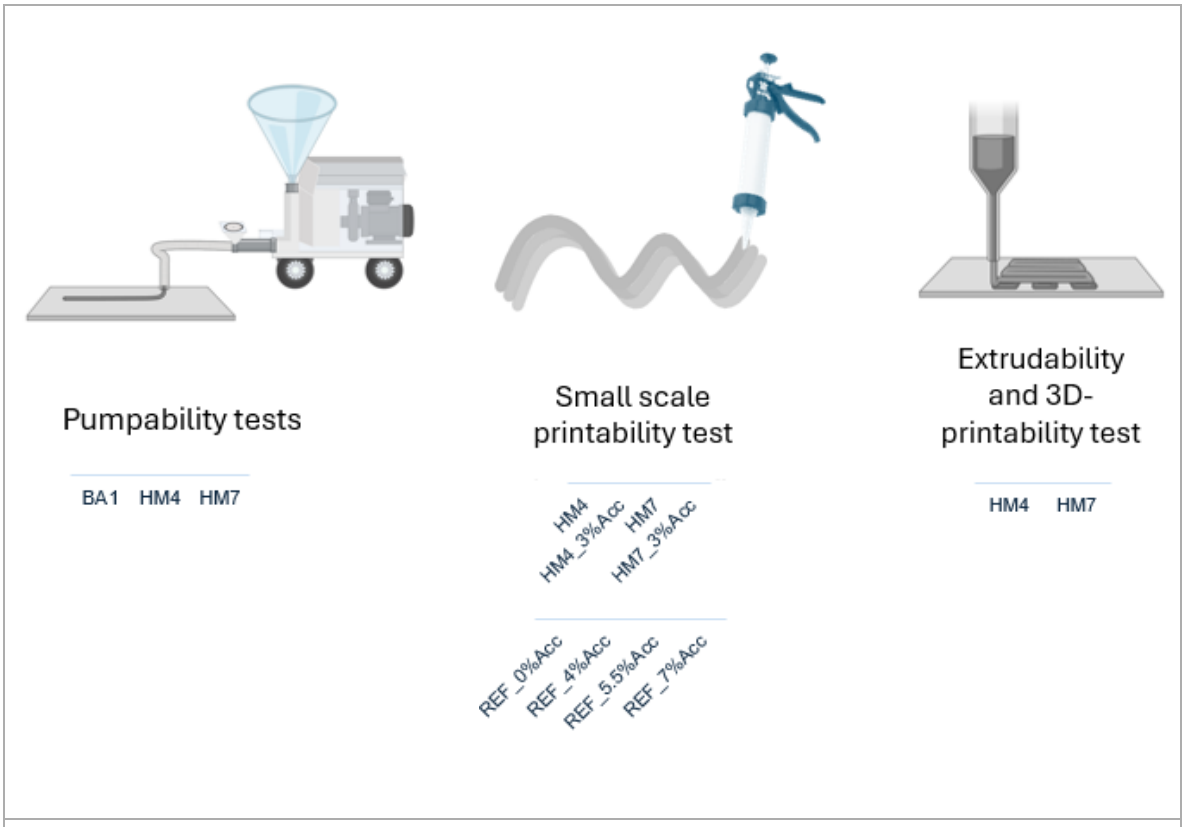

Figure 10 Schematic illustration of the printing test procedure and the corresponding samples for each mixture (created with biorender)

5.4.1 Pumpability tests

The pumpability of the mixtures was determined through pump tests with a spiral pump (MAI 2PUMP PICTOR-3D) [36] (Figure 10). Three mixtures: BA1, HM4, and HM7 with 6 litres (l) of volume were prepared and mixed with a high-capacity mixer. Following the mixing procedure described in Chapter 5.2.4. The pump setup was assembled according to Figure 10. After mixing, the fresh material was transferred into a funnel (max. 40 l capacity) and pumped through a tube to assess its pumpability. A small portion of each mixture was also cast into prisms for later strength testing (see Strength development). The results of these try-outs are visible in Chapter 6.

5.4.2 Small scale printability test

The printability of the AAM mixtures was evaluated through small-scale 3D printing trials using a silicon pump(Figure 11). Two sets of trials were carried out: four paste mixtures prepared using the overhead mixer (see Chapter 5.2.2), and six mortar mixtures prepared using the Hobart mixer (see Chapter 5.2.3). For each trial, approximately 500 ml of fresh material was placed into a silicon pump and extruded to evaluate printability (Figure 17). In total, eight samples were tested four reference mixtures with 0 %, 4 %, 5.5% and 7 % accelerator (ACC), and two AAM formulations HM4 and HM7 with 0% and 3 % ACC. The trials aimed to determine the number of layers that could be successfully printed immediately after mixing. Layers were successively extruded to evaluate the buildability and to identify the maximum number of layers achievable before failure. Results of the printability tests are presented in Chapter 6.

Figure 11 Typical set up for try-out with the silicon pump, silicon pump filled with sample

5.4.3 Extrudability and 3D- printability test

The 3D- printability of the mixtures was examined at a try-out with a 3D printer (WASP 40100 LDM)[37], [38]. This application setup was conducted following the established protocols for clay extrusion and 3D-printing [38].The purpose of this set up was to test how and if the material was printable with a 3D-printer, the typical set up is visible in Figure 12. Two mixtures HM4, and HM7 were prepared. Prior to the 3D printable test, the mixtures were mixed using a drill with paddle attachment (5.2.5) and then filled in the aluminium tank. Before printing, the extrudability of the mixture was tested shortly, as shown in Figure 13. It was checked to ensure that the mixture did not leak and was extrudable. Extrudability is a

requirement for printing. After the extrudability test was tested the pressure parameters were adapted, according to the needs of each mixture[38]. The results of these try-outs are visible in Chapter 6. The results of this try out are visible in section 6.2.3. After the printing try-out test runs, the samples were covered with foil to prevent drying out.

Figure 12 Typical set up for try-out with the 3D-printer

Figure 13 Extrudability test of HM4

6 RESULTS AND DISCUSSION

6.1 Physiochemical behaviour of the mixtures

6.1.1 Workability and rheology

Initial paste-level mixtures

The initial paste-level mixtures served to preselect suitable mixtures, which were determined based on the visual qualitative assessment of workability and mechanical properties(see 6.1.2) These workability tests showed that the pure metakaolin paste system exhibited insufficient workability, whereas the blended metakaolin- GBFS systems showed significantly improved the consistency and cohesion of the paste mixture.

Slump test

Basic mortar formulation with varying rheological modifier dosage

The slump test values for the basic formulation with varying rheological modifier dosage (BR1-BR6), are visible in Figure 14. The basic formulations, with varying rheological modifier dosage (0.5-1.3 wt.%), revealed that mix designs with high amounts of rheological modifier showed lower flowability, and a higher thixotropic behaviour compared to the mixtures with lower dosages. This is consistent with previous studies on AAMs, in which increased rheological modifiers, reduced initial flow but improved dimensional stability and structural development [39], [40].

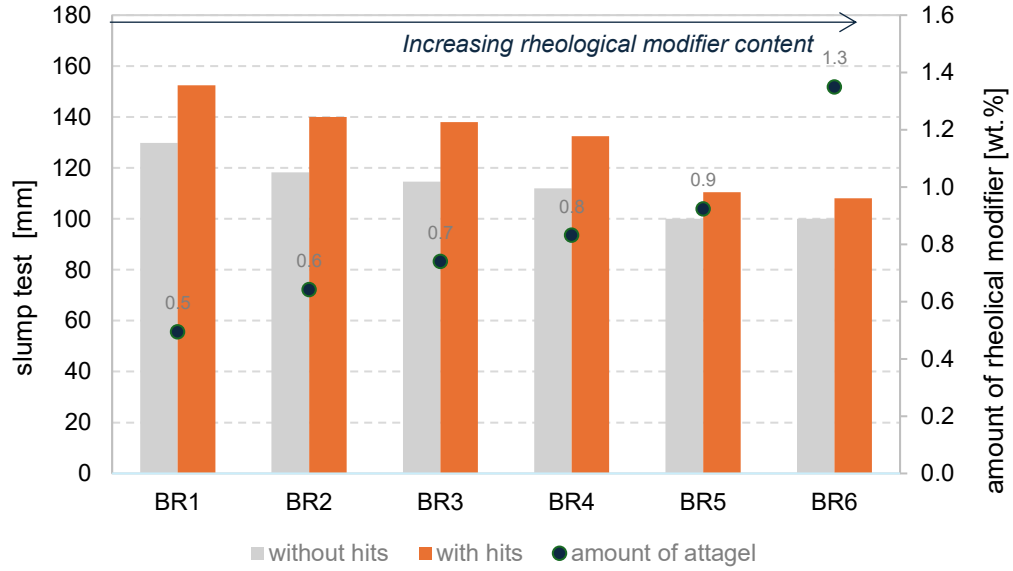

Figure 14 Slump test results of the basic formulation with varying rheological modifier dosage without and with hits

Basic mortar formulation with varying aggregate content

The basic mortar formulation with varying aggregate content (41.2 - 51.8%wt.) (BA1-BA3), the values of their slump test are visible in Figure 15. The flow and spread values of these mixtures revealed that with increasing aggregate content the flowability decreased.

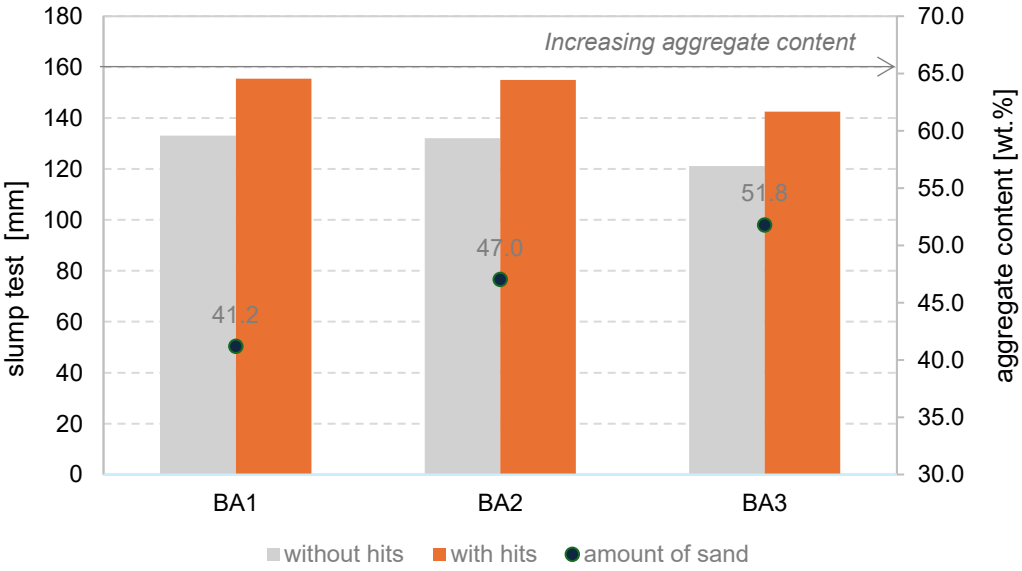

Figure 15 Slump test results of the basic formulation with varying aggregate content without and with hits

MK- GBFS mortar formulations

The following Figure 16 presents the influence of GBFS on slump. The tested mixtures (HM1-HM3) differ in GBFS and M_O content. The slump results show that flowability increased with higher amounts of GBFS indicating an optimized workability. Furthermore, it was observed that the difference between slump without hits and with hits had a significant effect on the flowability. HM3 with higher GBFS dose showed improvement of workability of the mortar mixtures especially when slump with hits was conducted. Figure 18 presents the results of the slump test for the mixture HM3-HM5 with different fluid contents. Both slump tests, with and without hits show a significant trend with changing fluid content, similar to figure 17 the values are higher when the test was performed with hits, contributing a positive effect on thixotropic behavior. Furthermore, the flowability decreased significantly with lower fluid content.

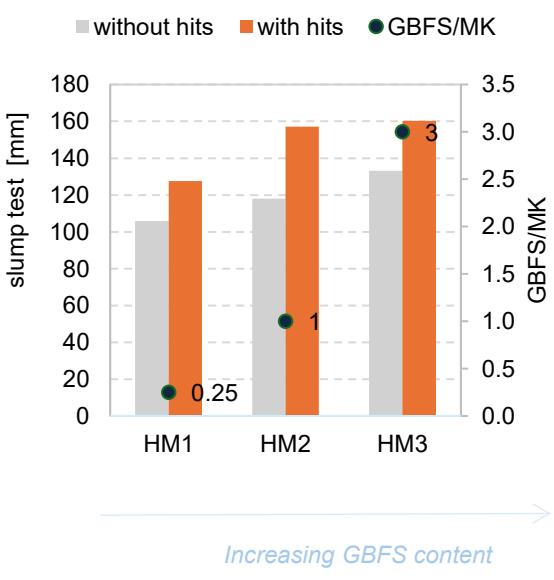

Figure 16 Slump test results of MK-GBFS mortar mixtures with varying GBFS/MK content the effect of GBFS/MK substitution, measured with and without hits.

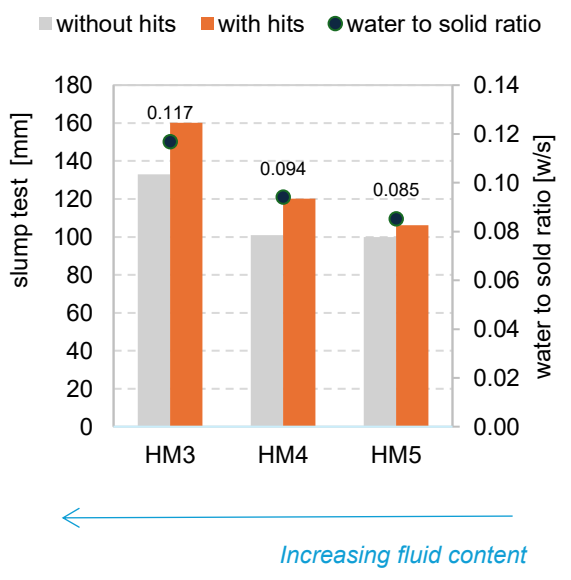

Figure 17 Slump test results of mortar mixtures with varying fluid content, measured with and without hits.

All slump measurement of the mortar mixtures (BR1- BR6, BA1- BA3, HM1- HM7) are compared in the graph below (Figure 18). In the literature, values of 115–200 mm were described as pumpable, extrudable, and printable for the application of 3D-printing [31]. The mixtures (BR5, BR6, HM5) with slump values with hits below 112 mm, exhibited poor flow and stickiness, while mixtures exceeding 157 mm (HM2, HM3) were overly fluid and therefore considered unsuitable for pumping and printing. Consequently, mixtures in between these values were considered as be pumpable. However, as discussed in section 6.2.1, the subsequent pumpability tests indicated that mixtures exceeding 155 mm showed excessive flowability and were not suitable for stable processing. Subsequently, the practical upper limit was altered to values below 155 mm. Based on the combined evaluation of fresh-state behavior, the optimal workability range was estimated to be between 115 and 130 mm.

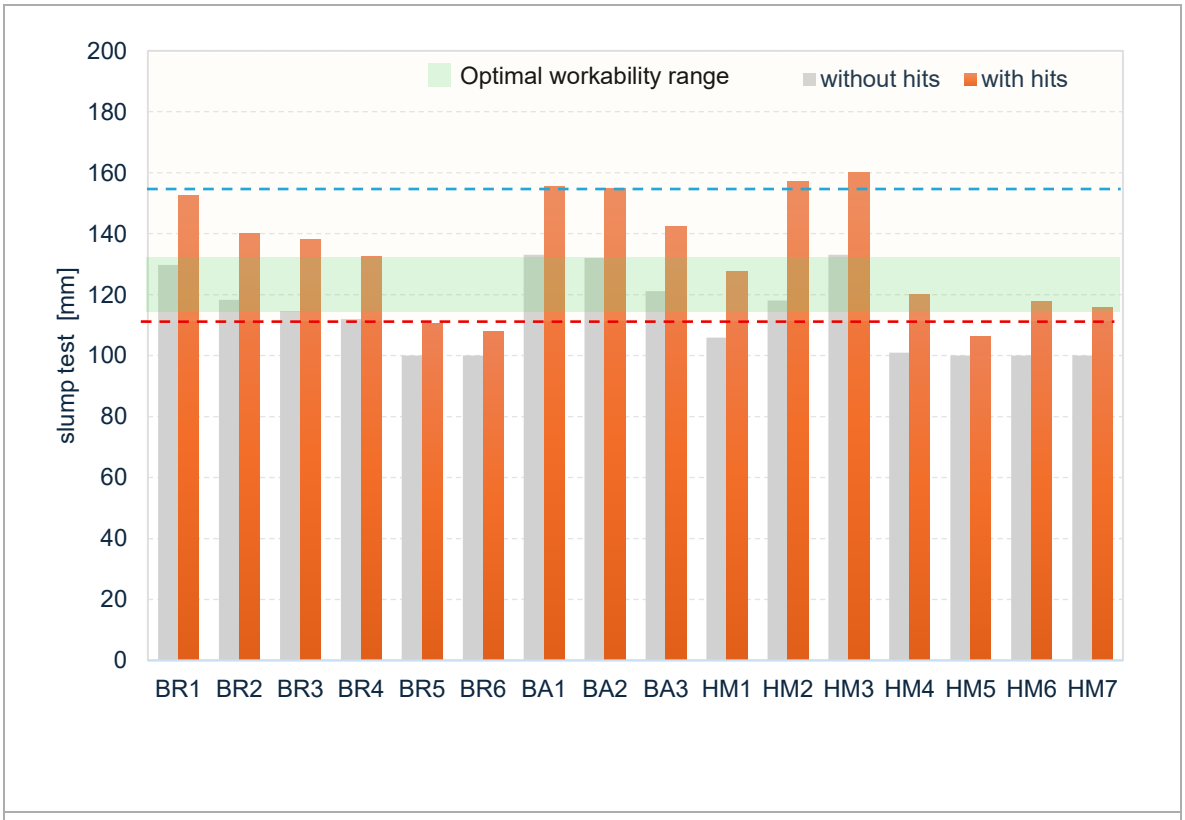

Figure 18 Comparison of the slump test in mortar development without and with hits

Impact of accelerator dosage on the setting time of selected mixes

The behaviour of the setting time of the different accelerated mixtures and corresponding reference mixtures (HM4, HM7) (HM4_3%ACC, HM7_3%ACC), as well as the reference material REF_ 5.5%ACC were tested with the Vicat needle. The results are shown for hybrid mixtures (HM4, HM7), accelerated mixtures (HM4_3%ACC, HM7_3%ACC) and the reference system (REF_5.5%). Furthermore, they were compared and evaluated.

Below in Figure 19, the Vicat needle test values of MK- GBFS based mixtures that combine basic and GBFS/MK-based formulations are presented. Both mixtures (HM4, HM7) without ACC show a continuous decline of penetration depth within 40-100 minutes. For the HM4 mixture the setting time starts earlier and a penetration depth of <5mm is reached after 75-80 minutes, for the HM7 mixture the hardening is significantly slower, <5mm is reached after 90-95 minutes.

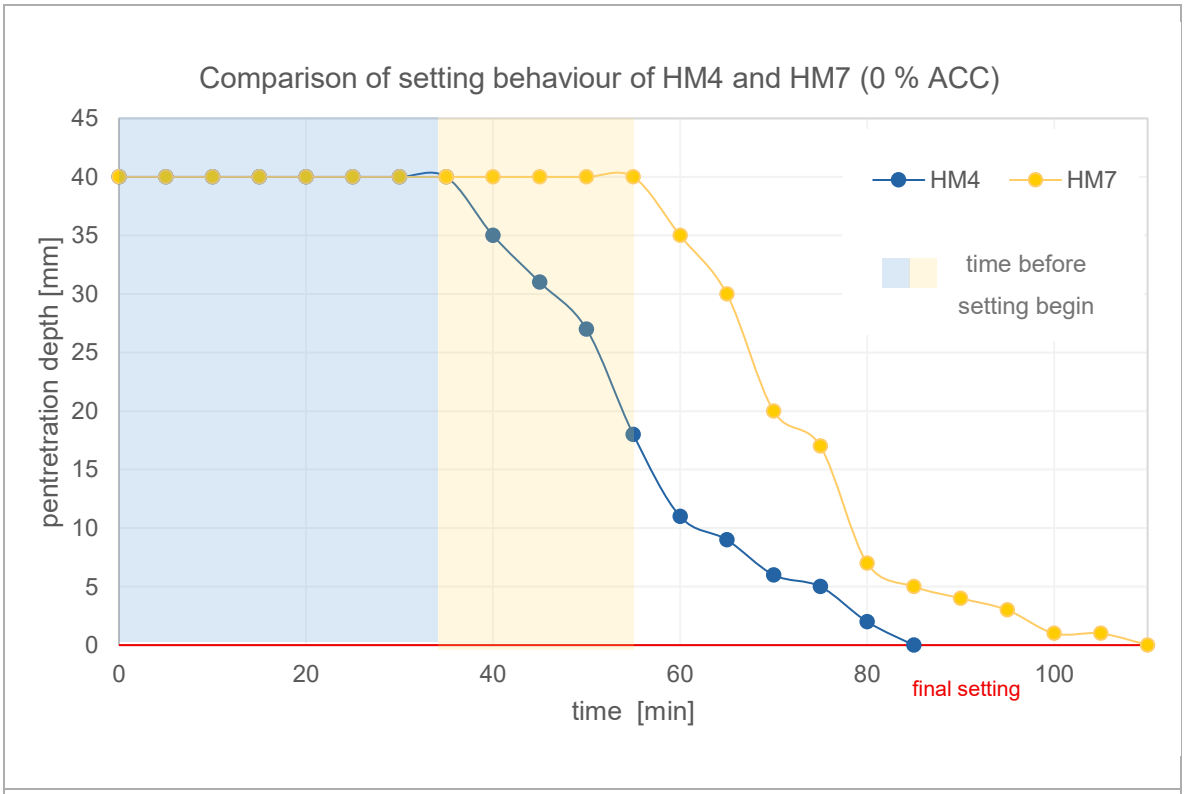

Figure 19 Vicat needle test of hybrid mixtures combining basic and GBFS/MK-based formulations

Below in Figure 20, the Vicat needle test values of ACC mixtures (HM7_3%ACC, HM4_3%ACC) are shown. The ACC mixtures show a continuous decline of penetration depth within a period of 30- 90 min. A penetration depth of <5mm for HM4_3%ACC was reached between 55-60min and HM7_3%ACC after 80-85min. Below in Figure 21, the Vicat needle test values of reference mixtures are given.

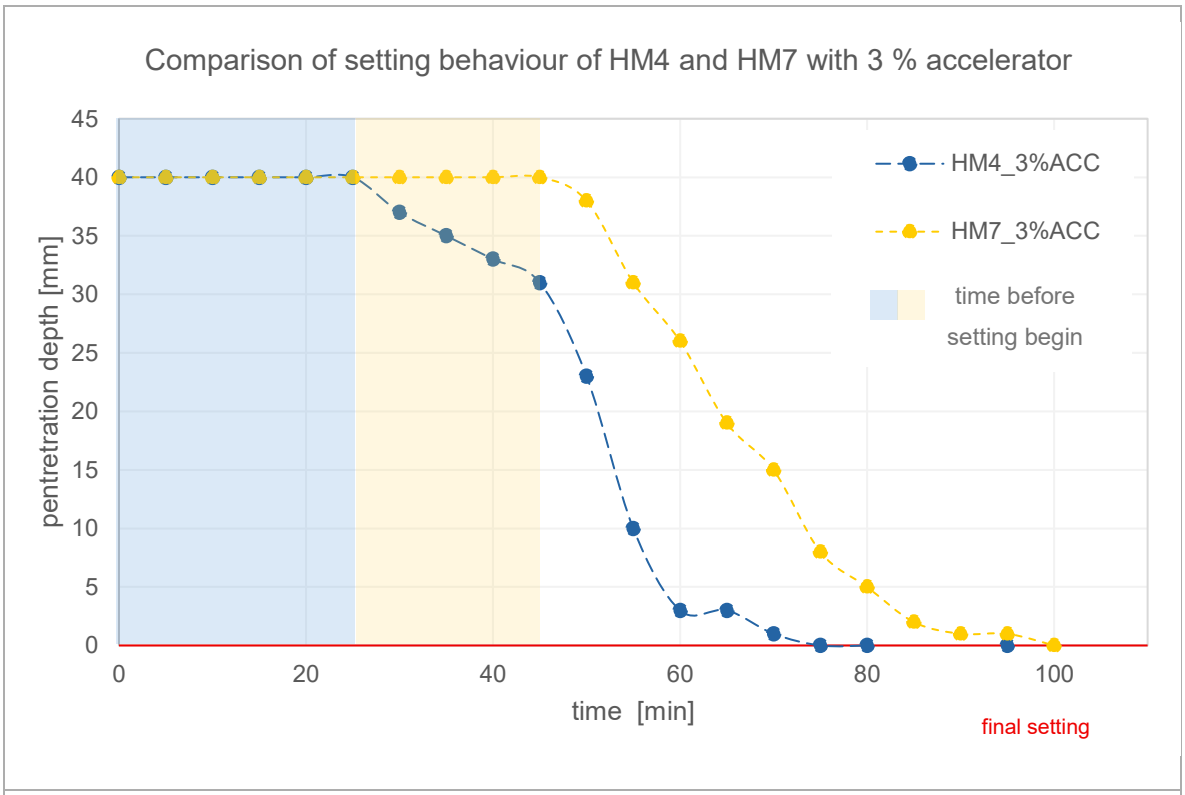

Figure 20 Vicat needle test of accelerated mixtures

Reference OPC mixture

For the reference mixture a continuous decline of penetration depth between 40-120 min occurred. A penetration depth of <5mm for REF_5.5%ACC was reached between 85-90 min. The final setting time was reached after approximately 155 min.

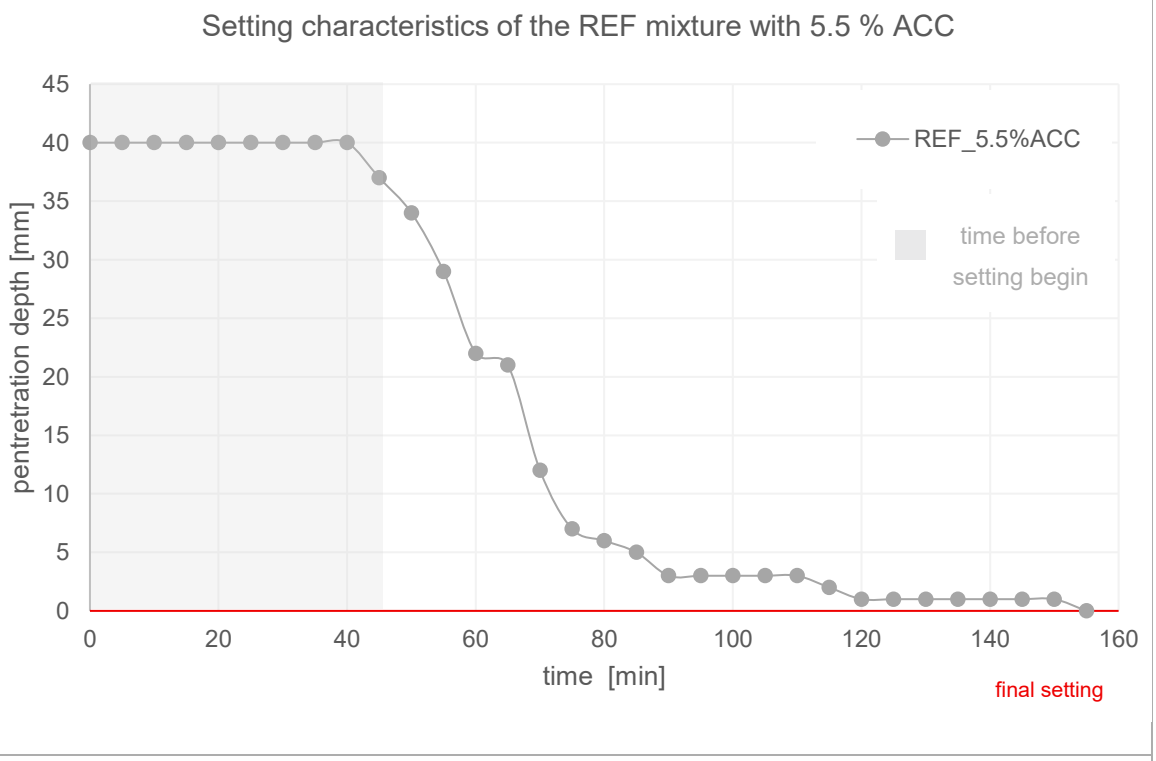

Figure 21 Vicat needle test of Reference mixture

Below in Figure 22, the Vicat needle test values of all tested mixtures are given and compared. The shorter setting time for both ACC mixtures (HM7_3%, HM4_3%) indicates the influence of ACC in both systems. It is further visible the HM4 system with and without ACC is shows faster reaction kinetics than the HM7 system. These differences suggest that the higher GBFS and specific aggregate content lead to faster structural development e.g. faster hardening. The accelerated mixtures of HM7_3%ACC, and HM4_3%ACC, show shorter setting times, which indicates the positive effect of the accelerator in respect to reaction kinetics and corresponding microstructural framework formation. The (REF_5.5%ACC) mixture required the most time to reach the final setting time although the initial setting start is similar to the other systems.

All following measurements, including setting time, strength development, were conducted using the reference value of 5.5 %ACC, as determined from the small scale printability tests described in section 5.4.2.

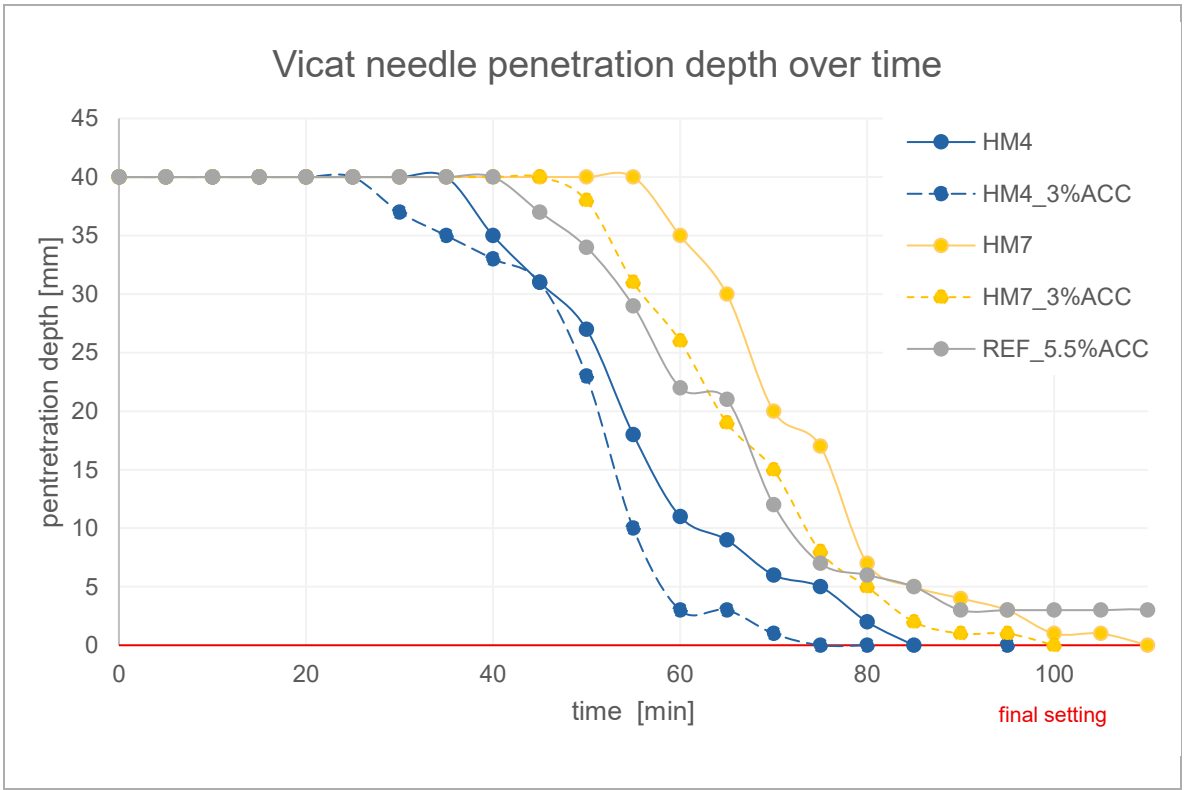

Figure 22 Comparison of the tested mixtures

6.1.2 Mechanical properties of the mixes

The behaviour of the strength development of a various number of different mixtures was tested. The results were compared and evaluated in the following chapters below.

Compressive strength

Initial paste-level mixtures

In Figure 23 the strength development of these basic pastes after 1 and 7 days are shown. In consequence of a slow reaction, poor compaction, and overly soft behaviour, it was not possible to measure the compressive strength of the mixture I1 after one day. After 7 days I1 shows a relatively low compressive strength of 12.6 N/mm² indicating that I1 is less suitable for applications requiring early strength development. However, I2 and I3 show significantly higher strength values after one day and seven days, suggesting that a blend of metakaolin M_O or M_R and GBFS as more suitable precursors for early strength development.

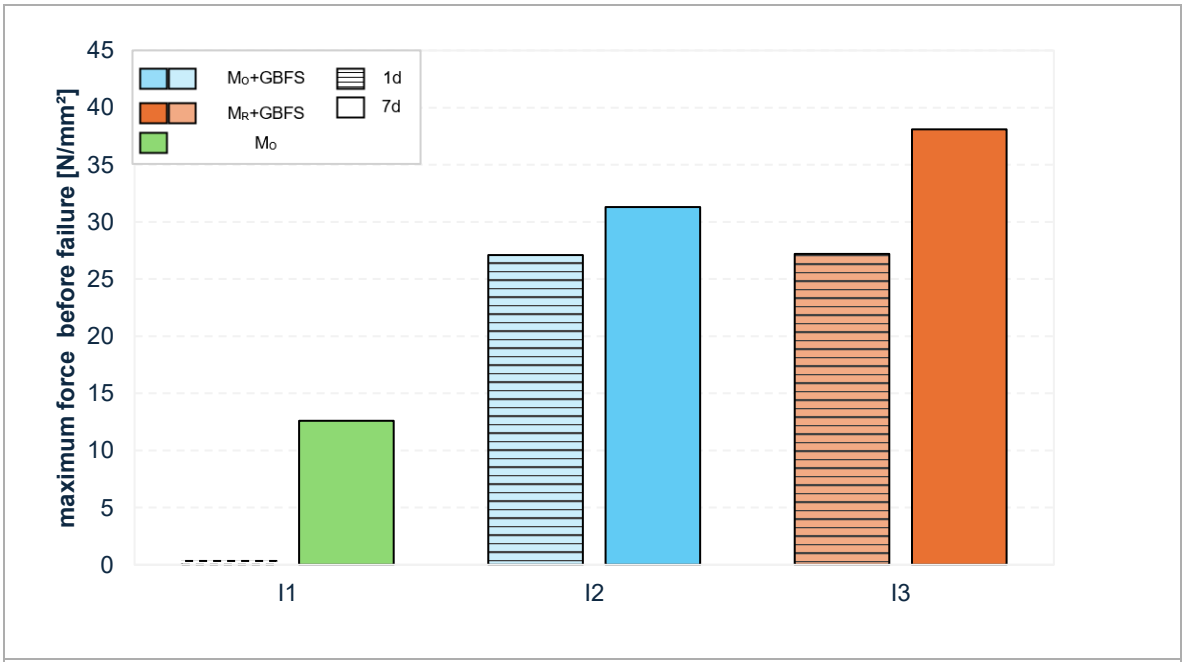

Figure 23 Compressive strength evolution of initial paste mixes after 1 and 7 days

Basic formulation with varying rheological modifier dosage

Strength development of BR5, BR6 with different amount of rheological modifier after 1 and 7 days are illustrated in Figure 24. The compressive strength values of BR6, with the highest amount of rheological modifier, indicate that variations in amount of rheological modifier influence the early and later strength of the mixture.

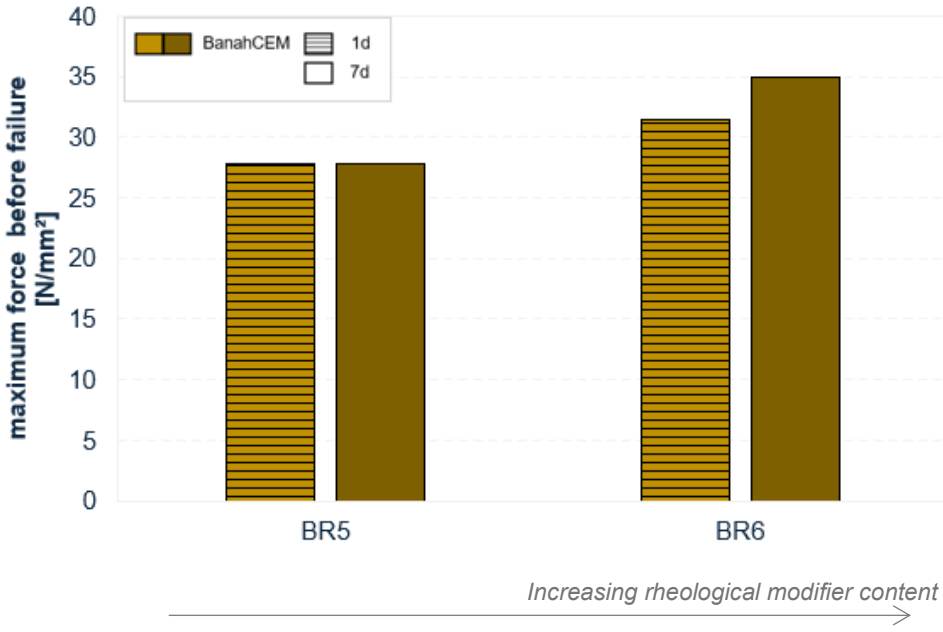

Figure 24 Compressive strength evolution of basic formulation with rheological modifier content wt.%. (0.9-1.3) after 1 and 7 days

Impact of binder – aggregate ratio on the mechanical mix properties

The evolution of compressive strength of the basic formulations with varying aggregate content is visible in Figure 25. Both mixtures BA2 and BA3 with higher aggregate content than BA1, show stepwise increase of compressive strength, indicating that an increase of aggregate content leads to a higher compressive strength; this might be due to increased packing density.

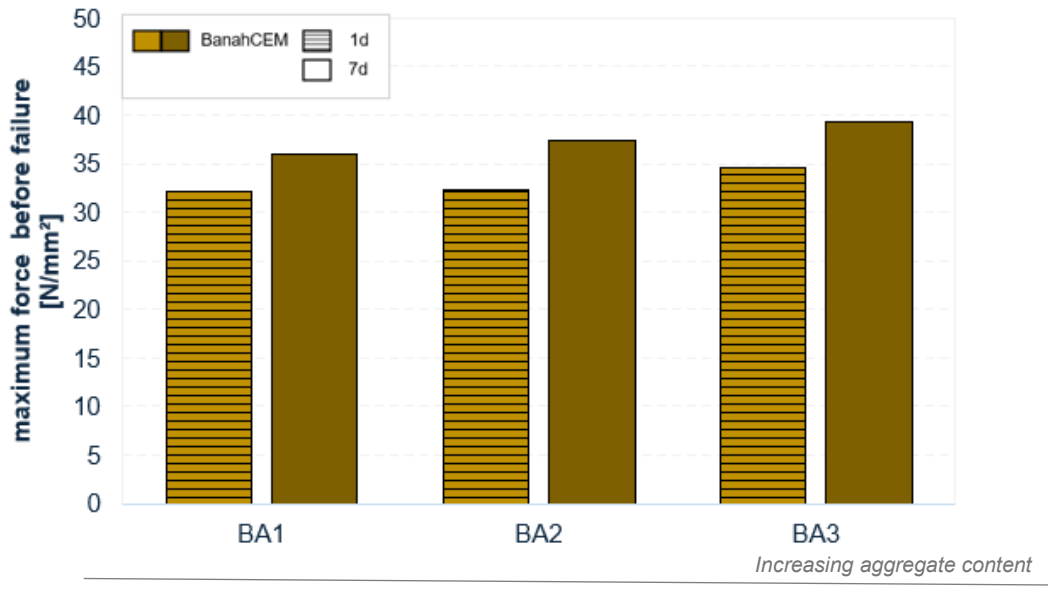

Figure 25 Compressive strength evolution of basic formulation with varying aggregate content 41.2-51.8 [wt.%] after 1 and 7 days

Impact of accelerator on the early strength development of blended MK-GBFS mixes

Early-stage compressive strength of the HM7 mix containing was tested for mixtures containing 0%, 3%, 5% and 7% accelerator at curing times of 3, 6, and 24 hours is shown in Figure 26.

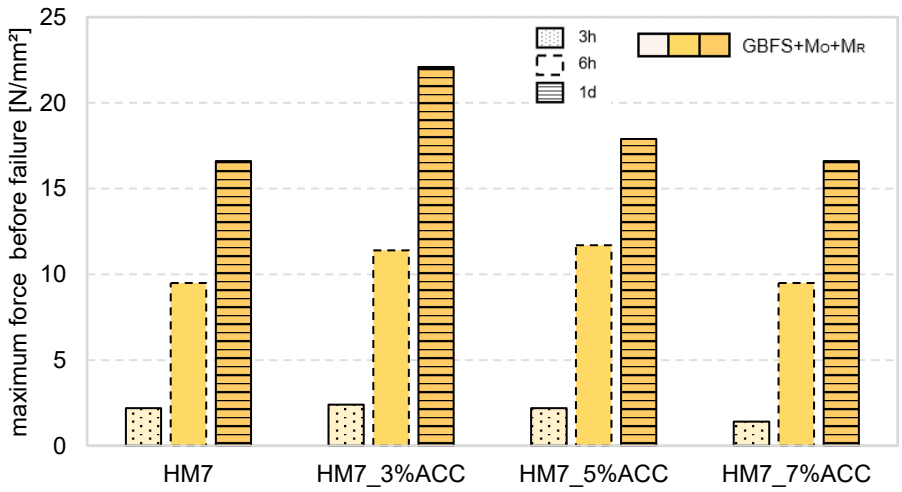

Figure 26 Early strength of mixtures after 3h 6h and 24h

As indicated by the measured early strength values of the HM4 and HM7 with different amounts of ACC (3%, 5%, 7%). HM7 without accelerator shows an increased in strength within 24 hours, indicating a successful reaction. In HM7_3%ACC, the strength values are slightly higher after 3 hours, and the strength continues to rise until 24 hours. By contrast the values of HM7_5%ACC (2.2 N/mm^2) and HM7_7%ACC (1.4 N/mm^2), after 3 hours are not higher, but rather at the same level or lower than for HM7 (2.2 N/mm^2). This suggests that the higher dosage of accelerator does not clearly benefit the system, however the difference is minimal. In Figure 27 the early strength results of the HM4 mixture with different amounts of ACC (3%, 5%, 7%) are illustrated.

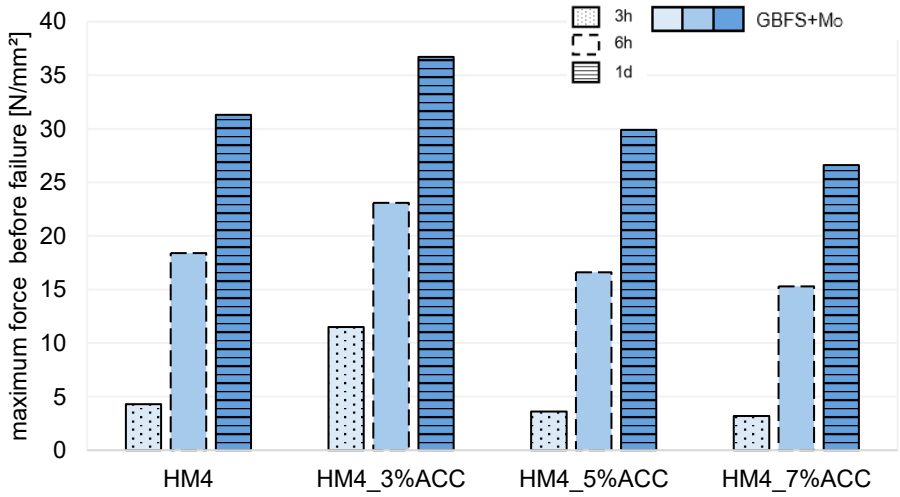

Figure 27 Early strength of mixtures after 3h 6h and 24h

As shown by the measured strength values, it can be assumed that the addition of accelerator influences the system. While HM4 without accelerator shows a steady increase in strength within 24 hours, HM4_3%ACC, exhibits the highest strengths in all three categories, 3 hours (11.5 N/mm^2), 6 hours (23.1 7N/mm^2), 24 hours (36.7 N/mm^2). This is particularly evident after 3 hours, which indicates a successful accelerated system. Contrary to expectations, HM4_5%ACC and HM4_7%ACC do not exceed this, but rather lower strength values are observed. At 3 hours, 6 hours and after one day, the values of HM4_5%ACC and HM4_7%ACC are even lower than those of the initial mixture HM4. Since HM4_5%ACC and HM4_7%ACC had lower strengths than the initial mixture, it can be assumed that the increased addition of the accelerator has either led to an unbalanced chemical composition (Na and/or Al overdosage) or a very early and thus not recorded

overreaction resulting in disturbed microstructure development and consequently lower strength. It is important to note that the higher dosage of ACC does not necessarily improve the quality of the mix design. Both mixtures containing 3% ACC (HM4_ 3%ACC, HM7_ 3%ACC) showed the highest compressive strength; therefore, further tests were carried out with 3% ACC, which was considered the optimum ACC dosage.

Compressive strength was tested for mixtures HM7and HM4 at curing time after 7 days. Both mixtures show similar strengths after 7 days: HM7 with 55.2 N/mm² and HM4 with 55.6 N/mm². The following graph (Figure 28) shows the strengths of the reference mixture.

Reference mixtures

Compressive strength was tested for the reference mixtures with 0 % 4% and 5.5% ACC curing time after 7 days in values are visible in Figure 28. This figure shows that the strength values are influenced by the accelerators. REF (without ACC) has the highest value with 42.6 N/mm², REF_4%ACC has the lowest value with 37.2 N/mm² and REF_5.5%ACC reached 40.1 N/mm² after seven days. REF_5.5%ACC is slightly higher than REF_4% but lower than REF. At REF_7%ACC, it hardened so quickly in the practical test with the silicon pump (Chapter 6.2.2), that the mixture was not further tested. To compare the developed (HM7, HM4, BA1) and the reference mixture (REF with different amount of ACC (4%, 5.5%), they were displayed in the same plot (Figure 28).

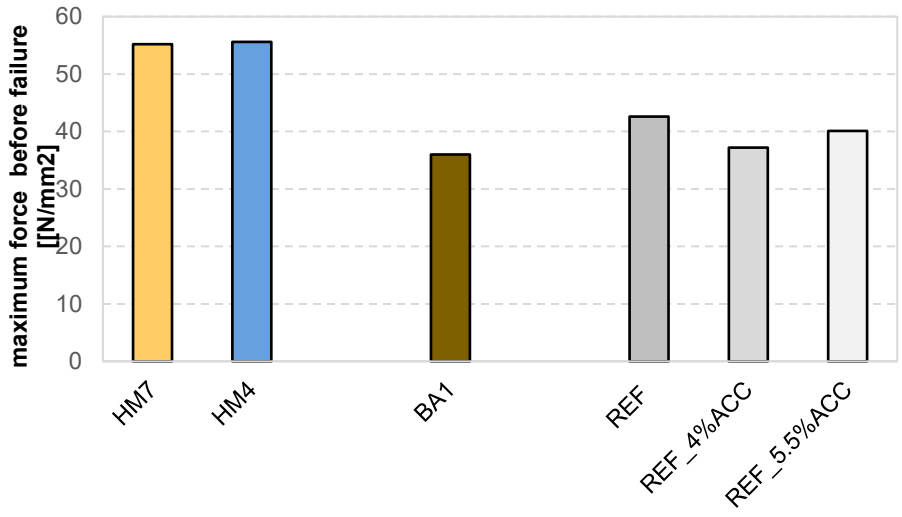

Figure 28 Compressive strength values of BA1, HM4 HM7 and REF mixtures with and without ACC (0, 4%, 5.5%) after 7d

The comparison of the reference material with the developed material (BA1, HM7, HM4) shows that the developed mixtures (HM7, HM4) not only match the performance of the reference mixture but even achieved superior compressive strength values after 7 days. BA1 did not meet the required criteria to at least achieve the same strength as the reference material and was therefore and due to time limitations not further investigated.

Tensile strength

Basic formulation with varying rheological modifier dosage

In Figure 29, the tensile strength development of the basic formulation with varying rheological modifier dosage of the mixtures BA5, BA6 after 1 and 7 days are shown.

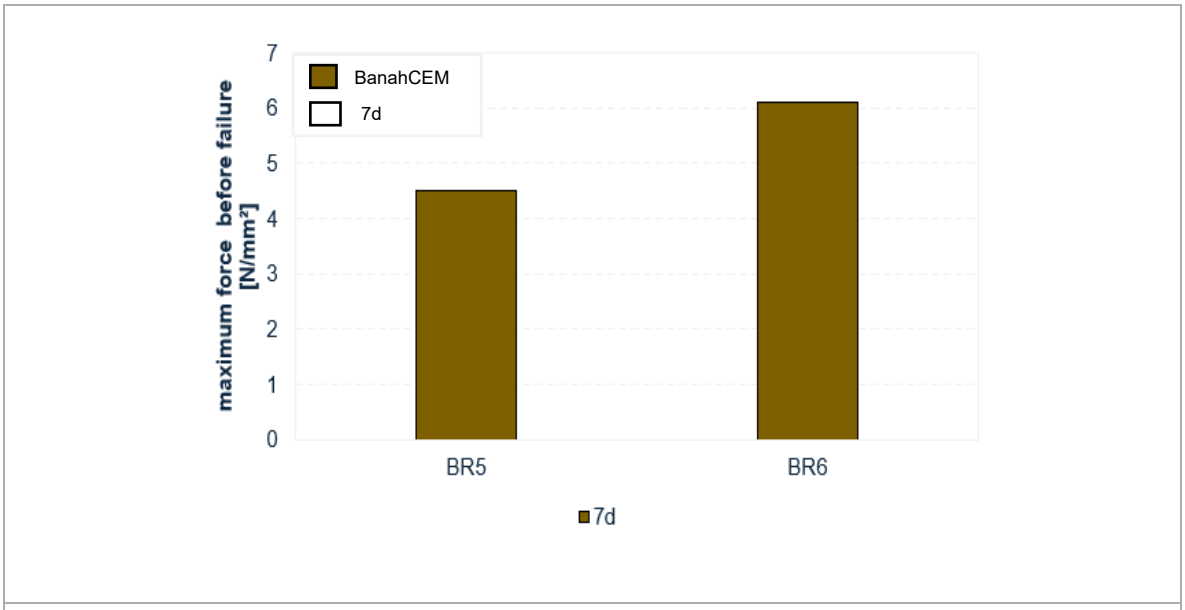

Figure 29 Tensile strength evolution of the basic formulation with varying rheological modifier dosage after 1 and 7 days

Basic formulation with varying aggregate content

Figure 30 demonstrates the strength evolution of these basic mortars BA1, BA2 and BA3 with different amounts of aggregates after 1 and 7 days. It is visible that the mix with the highest number of aggregates represented by BA3, shows the best result, e.g. highest strength values.

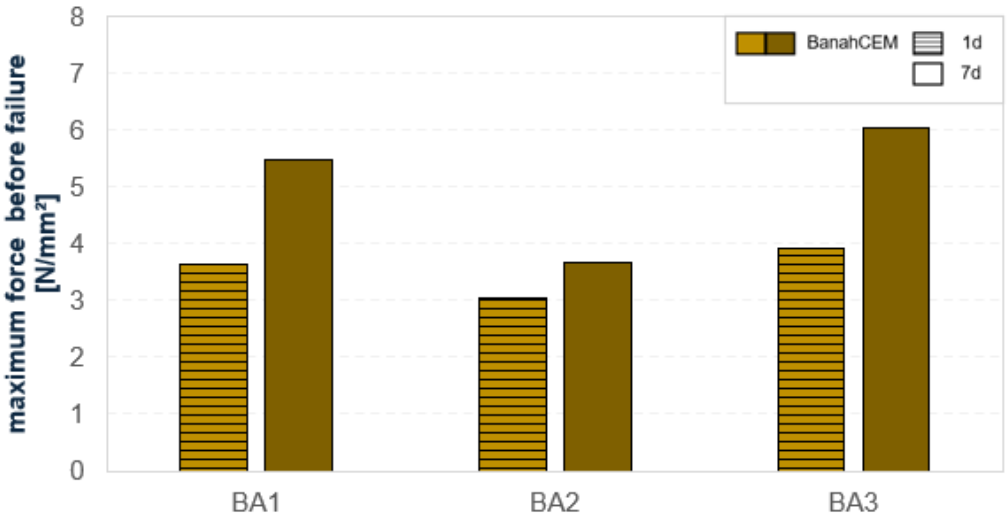

Figure 30 Tensile strength evolution of basic formulation with varying aggregate content after 1 and 7 days

Developed mixtures (HM4, HM7, BA1) vs. the Reference mixtures (REF, REF_4%ACC, REF5.5%)

In Figure 31 the strength development of the different mixtures after 7 days is presented. The mixtures HM4 and HM7 show higher values with approximately 7.4 - 8.8 N/mm² exceeding, the reference mixtures REF, REF_4%ACC and REF_5.5%ACC. The mixture HM4 has the highest strength development after 7 days with approximately 8.8 N/mm². The mixtures REF, REF_4%ACC and REF_5.5%ACC achieved tensile strengths after 7 days between 5.0 -7.3 N/mm². BA1 did not meet the required conditions to at least achieve the equal strength as the reference material, consequently the mixture BA1 was not further investigated.

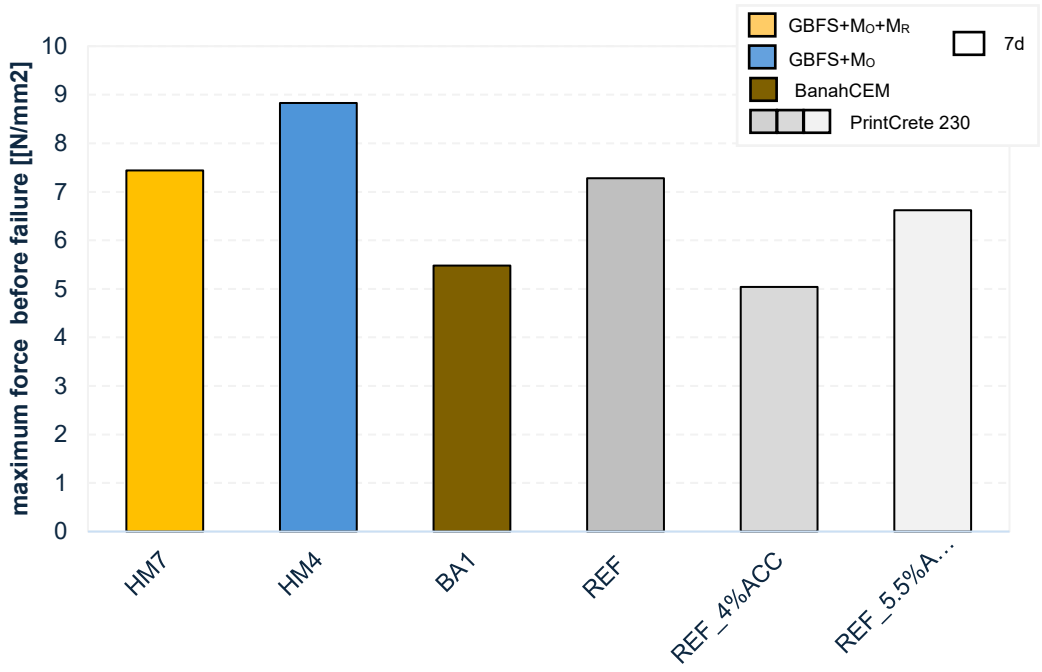

Figure 31 Tensile strength of BA1, REF with and without ACC and GBFS/MK-based formulations

6.1.3 Heat development

Hybrid mixtures combining basic and GBFS/MK-based formulations (non-accelerated mixtures) & accelerated mixtures

In this section the results from the calorimeter measurement are shown and discussed. The cumulative reaction heat development (J/g of binder) as a function of time after mixing for two AAM systems (HM7 and HM4) each tested with and without an accelerator (0% and 3%), is shown in Figure 32.

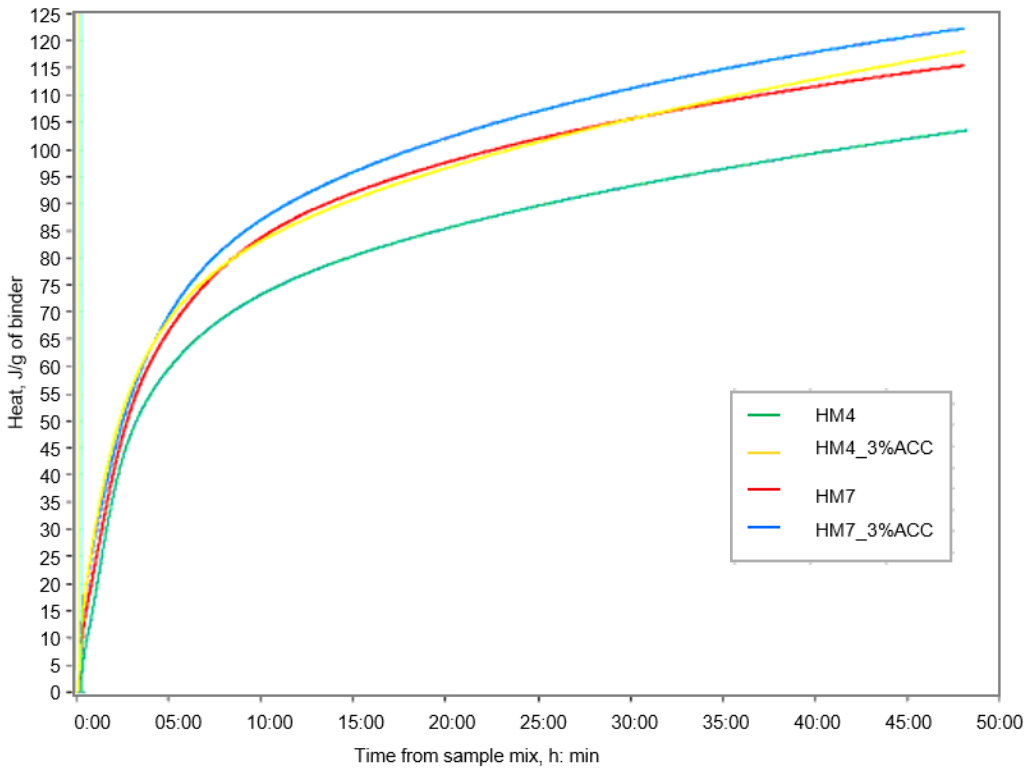

Figure 32 Cumulative heat flow per g of binder in 48h

During the measurement, all four curves exhibit a continuous heat increase, representing the ongoing alkali-activation reaction processes of the samples. Both accelerated mixtures HM4_3%ACC and HM7_3%ACC exhibit higher cumulative heat release compared to the non-accelerated samples (HM4 and HM7). This might indicate a stronger and faster early and overall reaction due to the acceleration process. Within the non-accelerated samples, HM7 shows higher reaction heat release than HM4, signalling that mixture HM7 is inherently more reactive under the given curing conditions. The accelerated sample HM7_3% reaches the highest cumulative heat development after 48h (123J/g) of all mixtures, exceeding both HM4 (118J/g) and the non-accelerated mixtures HM7 (115.5J/g), HM4 (104J/g). This data indicates that the HM7 system shows slightly higher total reactivity than the HM4 system, and that the use of an accelerator significantly enhances the early alkali-activation reaction in both AAM formulations. In addition, the cumulative heat flow, the thermal power in relation to the solid ratio (W/g binder) was plotted to further determine the differences in reactivity of the mixtures. Therefore, in the following Figure 33 the graph for the thermal power with W/g binder for all four mixtures in 48h are presented.

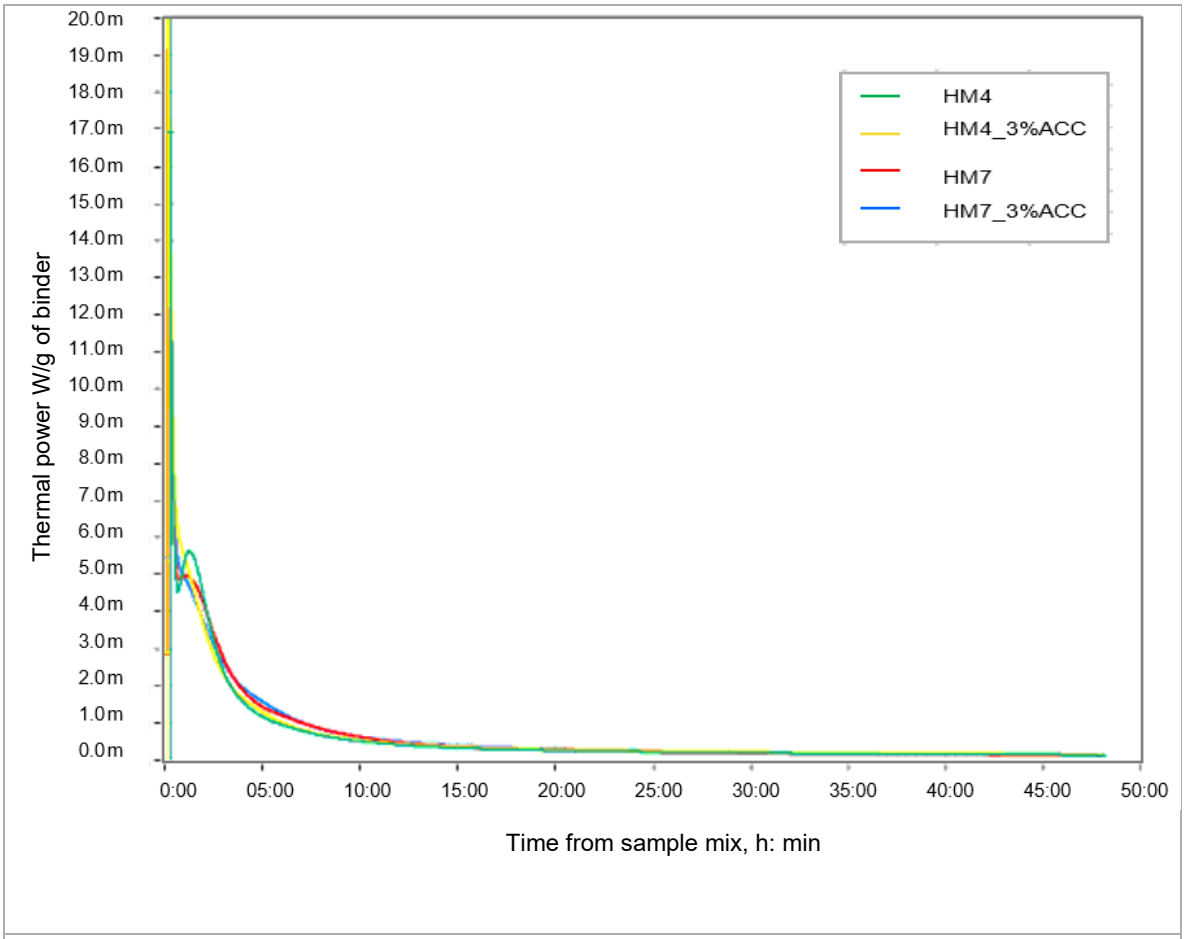

Figure 33 Thermal power with W/g binder (solids) for the timespan of 48h

The previous graph Figure 34 illustrates that all mixtures exhibited the highest thermal output in the first five hours after mixing. Therefore, in Figure 34 and Figure 35 provide a detailed look into this specific time period. An initial exothermal peak (Peak 1) occurred within the first 30 minutes for all samples, representing the rapid dissolution and early gel formation phase. In the first phase of alkali activation processes, the particles react quickly with the alkaline solution. This results in intense exothermic processes that often cannot be accurately recorded by the calorimeter, as the device is sensitive to rapid reaction changes and has technical limitations[41]. The first peak was significantly higher for the accelerated mixtures HM4_3%ACC (yellow) and HM7_3%ACC (blue) than for the non-accelerated HM4 (green) and HM7 (red) indicating that the accelerator increased reaction kinetics. After approximately 35– 40 minutes, the heat flow declined significantly for all mixtures. A secondary, smaller peak (Peak 2) appeared only in the non-accelerated mixtures (HM4, HM7), while it was absent in the accelerated ones. The accelerated mixtures (HM4_3%ACC,

HM7_3%ACC) released most of their heat during the early reaction phase, after which the heat flow rapidly decreased and remained low for the rest of the measurement. However, the non-accelerated mixtures showed a slower reaction pattern with a secondary increase in thermal power, suggesting further condensation processes. The significant first peak and suppression of the secondary peak in accelerated mixtures HM4_3%ACC and HM7_3%ACC are consistent with other calorimetric profiles of accelerator-modified GBFS systems, in which an early rapid reaction consumes most of the reaction potential [42], [43].

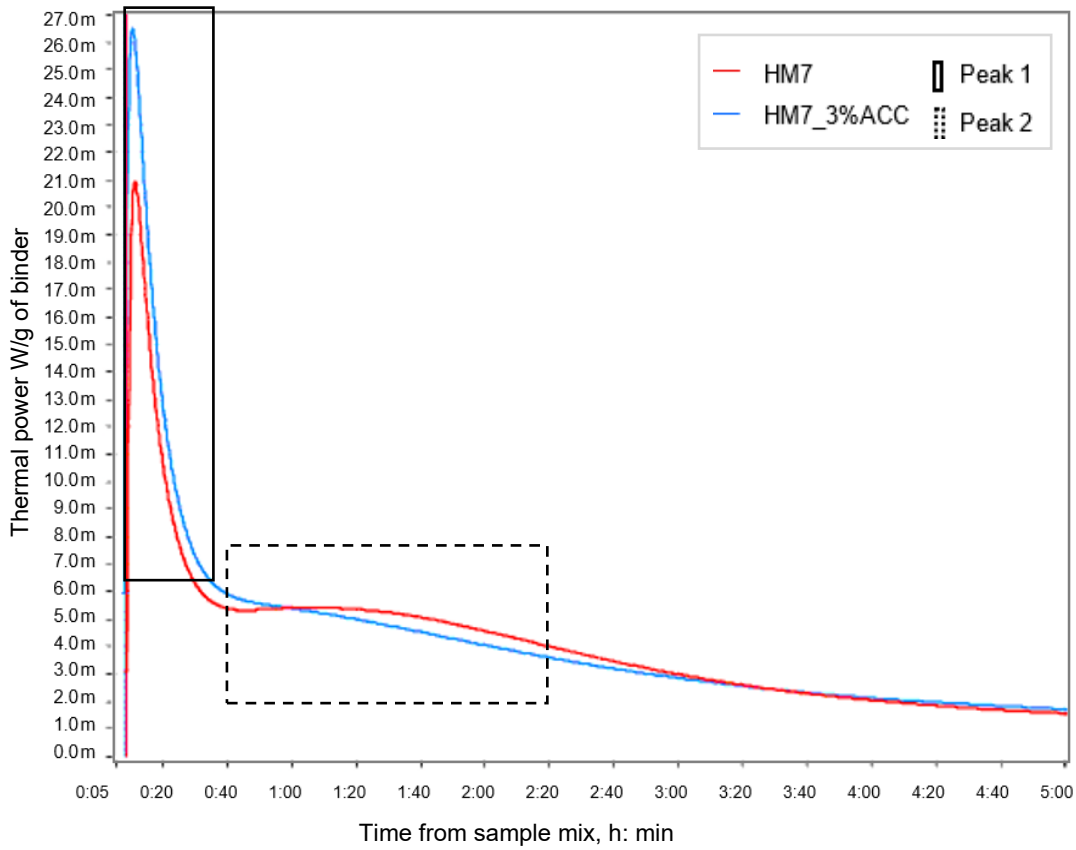

Figure 34 Thermal power with W/g binder for the timeframe of 5h for HM7 and HM7_3%ACC

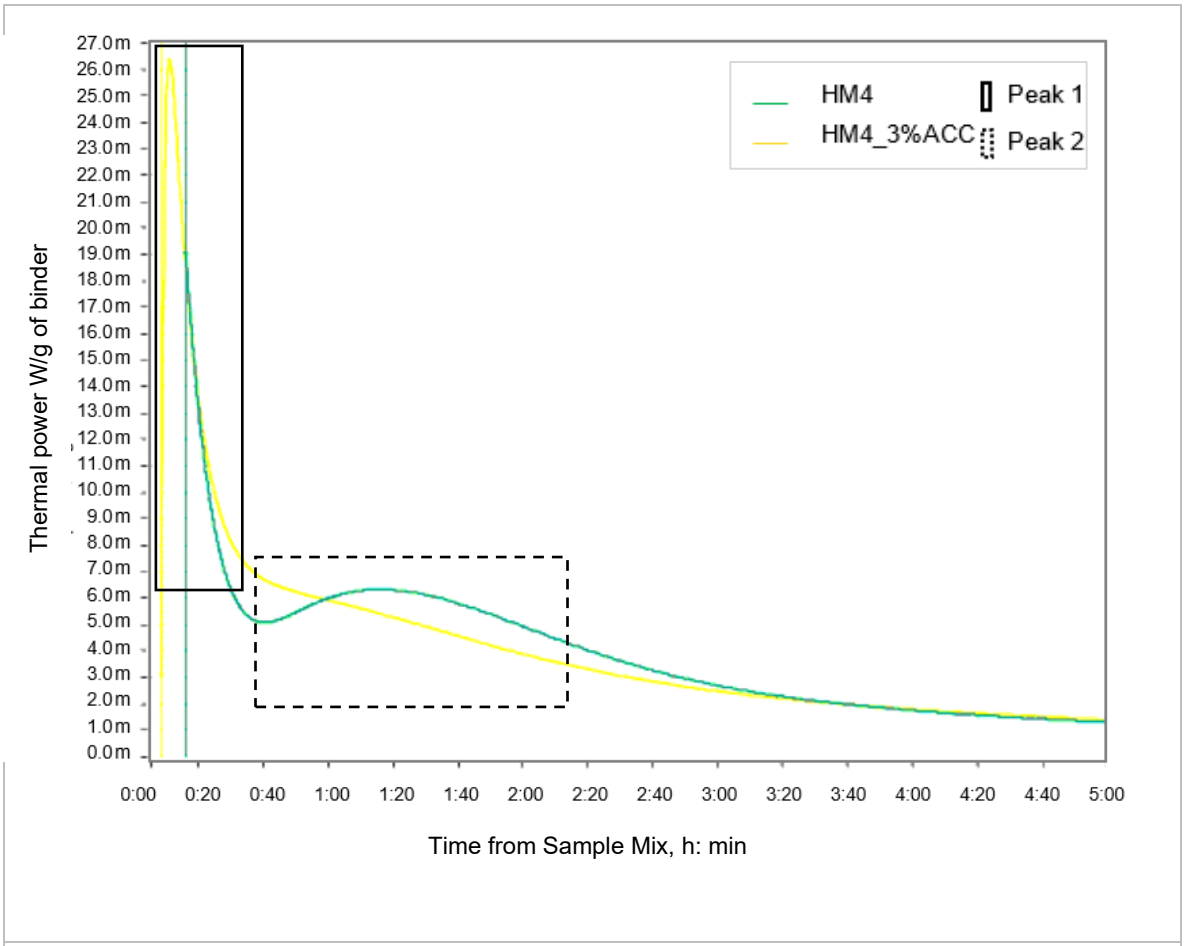

Figure 35 Thermal power with W/g binder for the timeframe of 5h for HM4 and HM4_3%ACC

The non-accelerated mixtures (HM4, HM7) indicate a lasting reaction activity and a controlled heat release, suggesting a stable alkali activation process. The first peak in the reaction for MK- rich systems describes the dissolution and the second the gelation and framework formation[44]. The secondary more pronounced peak of HM4 compared to HM7 is due to the higher Metakaolin content, which benefits an aluminosilicate dissolution and further polymerisation. In systems with GBFS and MK the secondary production of heat can emerge from reaction products of C-(N/K)-A-S-H. In HM7 the slightly higher the GBFS content and silica availability, indicating faster Ca- dominated reactions and partially overlapping of dissolution and precipitation stages leading to a less distinct second peak [44]. The results of the measurements of the accelerated mixtures indicate an acceleration effect on HM4_3%ACC and HM7_3%ACC, which is observable in the form of a higher first peak and repressed lower second peak, but that does not mean that the acceleration is a requirement for processing. Hence, the accelerator influences the timing of the heat release,

it is indicated that the reaction kinetics are affected by the usage of the ACC. The effects on pumpability and printability are discussed in the next section.

6.2 Pumpability and printability of the mixtures

In this chapter the results of the pumpability printability of the tested mixtures are presented and compared.

6.2.1 Pumpability

Performance of the basic formulation with varying aggregate content (BA1)

Mixture BA1 could be pumped and extruded continuously, demonstrating adequate pumpability. However, during the layer-build-up process, the material exhibited excessive flowability and insufficient structural stiffness (Figure 36). As a result, the deposited layers deformed and slid laterally, preventing stable stacking. This indicates a lack of buildability, which is considered a key requirement for extrusion-based 3D printing. BA1 showed strong adhesion to the wooden substrate, resulting in difficulties when removing printed elements. Therefore, a thin layer of oil was applied, on the substrate plate for the following try outs, as a release agent.

Performance with MK-GBFS based formulations HM4 and HM7

Both mixtures (HM4 and HM7) were extrudable and enabled stable stacking of at least three layers under the tested print conditions (Figure 36). It was noted that the usage of a different mixer (Compulsory Mixer), as well as the vibrant tool, added to the funnel, prevented the mixtures from getting stuck. This led to slightly increased flowability of the mixtures during the pumping process. Due to the limited produced sample volume, further evaluation of maximum build height was not possible within this try-out.

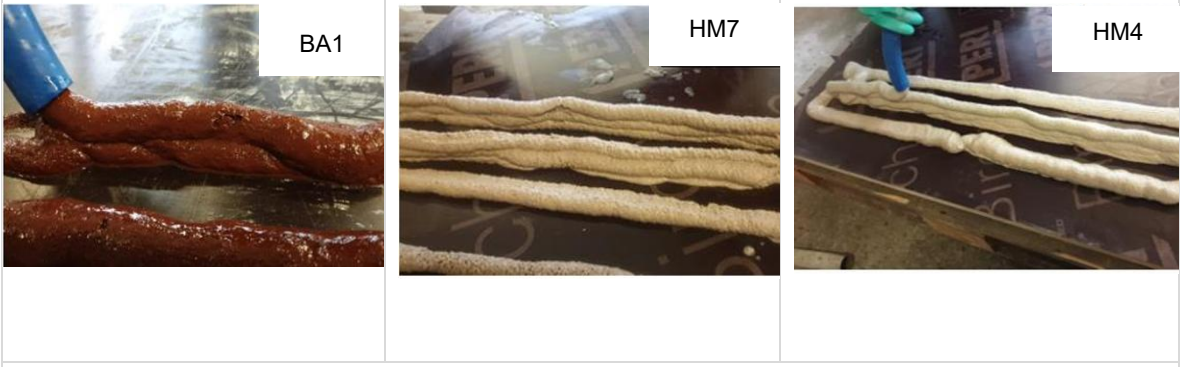

Figure 36 Mixture BA1 (left) showed high flowability, and insufficient structural stiffness, HM7 (middle) and HM4 (right) were extrudable and enable stable stacking of at least three layers under the tested print conditions.

6.2.2 Printing trials with a silicon pump

Performance of hybrid mixtures with GBFS/MK-based formulations HM4 and HM7 with and without ACC

The hybrid mixtures with GBFS (HM4 and HM7) were successfully extruded through the silicone pump. The results are summarized in Table 10, HM4 enabled the construction of nine stable layers without visible deformation. HM7 showed comparable printability, although lateral deformation occurred from the 6th layer onward, followed by a collapse during the 9th layer. Due to the limited testing setup, experiments could only be conducted in paste form, meaning that aggregates were not included in the mixtures, therefore a slightly excessive fluidity was exhibited for HM7_3%ACC. It is assumed that, under improved experimental conditions or after an extended resting period, the mixture would reach the desired viscosity. In contrast, the HM4_3%ACC mixture demonstrated good stability, allowing for the successful application of up to eleven layers. In contrast when mixture HM7_3%ACC as a mortar mixture was tested as a mortar mixture, a build-up of up to 9 layers was possible, but from the 7th layer on a lateral deformation was visible, followed by a collapse during the 9th layer. The HM4_3%ACC as a mortar showed a good stability and a build up to eleven layers was possible.

Performance of Reference mixtures

Table 10 Printability results of small-scale pump trials

Mixture	ACC type	ACC content [%]	Maximum number of stable layers	Observation
HM4	–	0	9	Good buildability; no collapse up to 9th layer
HM7	–	0	8	Layer deformation from 6th layer; collapse at 9th layer
HM4_3%ACC (paste)	SIKA Sigunit®L22	3	11	Good buildability; no collapse up to **11th layer**
HM7_3%ACC (paste)	SIKA Sigunit®L22	3	-	As paste to fluid for printing; no layer formation possible
HM4_3%ACC	SIKA Sigunit®L22	3	11	Good buildability; no collapse up to **11th layer**
HM7_3%ACC	SIKA Sigunit®L22	3	9	Layer deformation from 7th layer; collapse at 9th layer
REF	AdSpeed 200	0	-	Too fluid for printing; no layer formation possible
REF_4%ACC	AdSpeed 200	4	3	Collapse during 4th layer
REF_5.5%ACC	AdSpeed 200	5.5	5	5 possible layers, collapse after 5th layer
REF_7%ACC	AdSpeed 200	7	-	Rapid stiffening: pump blockage prevented extrusion

The reference mixture without accelerator (0% ACC) was highly fluid after its extrusion through the silicon pump and was consequently not printable. Hence, the manufacturer recommended dosage of ACC was between 4-7% ACC (manufacturer data Baumit PrintCrete system), mixtures with 4 % , 5.5% and 7% were invested. The mixture with 4% ACC allowed stacking of three stable layers before a collapse occurred during the fourth. The mixture containing 5.5% ACC enabled the deposition of five layers before deformation and a collapse occurred it yielded the best results within the manufacturer's range, was therefore chosen as the reference for comparison. The REF with 7% ACC stiffened too rapidly and caused a pump blockage, preventing any layer formation. Hence, the mixture was considered unprintable in the small test pump, it was not further invested. Compared to the reference system, the hybrid mixtures HM4 and HM7 exhibited superior buildability

under the same simplified test conditions. This suggests that the incorporation of GBFS enhances the early structural stability required for extrusion-based layer formation. These results (summarized in Table 10) underline the very narrow process window in extrusion-based AAM mixtures between too fluid and too stiff and highlight the importance of aligning material formulation with the specific pumping and deposition system used.

6.2.3 3D printing test

Performance of hybrid mixtures with MK- GBFS based formulations HM4 and HM7

In Table 11 the adapted printing parameters for each mixture are summarized, as well as the number of printed layers for each mix are shown. Due to some start delay during the experiments and the short workability window of the material, a limited number of layers on top of each other were possible, not presenting the maximum amount of layers possible from a material property point of view. It was also observed for both mixtures that the material stretches slightly when it comes out of the nozzle and trails slightly behind, which means that some layers do not lay exactly on top of each other. The printed layers for each material are presented in Table 11.

Table 11 Details of the prepared mixtures and their type and amount of accelerator as well as the number of printed layers

MIX	Used amount of pressure [bar]	amount of ACC [%]	number of layers	Observations
HM4	1.5	0	6	Printing was possible; initial pressure exceeded limit and was reduced during operation
HM7	5	0	7	Higher pressure required, likely due to increased aggregate content and partial blockage at the screw conveyor (8 mm nozzle)

Figure 37 Printing process of the HM4 mixture

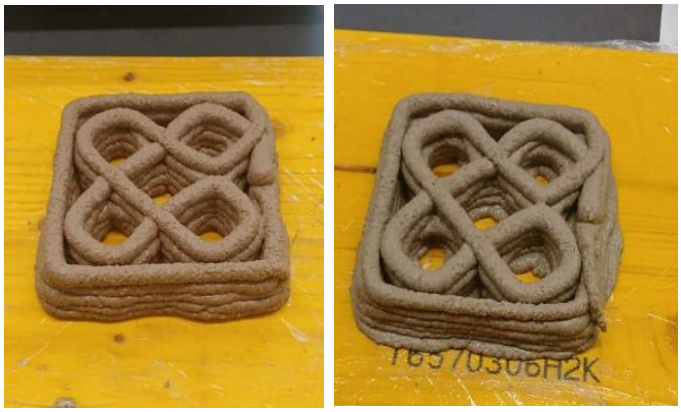

Figure 38 Printed layers of HM7(left) and HM4(right)

As this printer did not allow for an in-situ dosing of the accelerator at the nozzle head, the accelerated mixtures were not tested. The printing test with the developed mixtures HM4 and HM7 was largely successful and provided valuable insights for further possible optimization. Although the short processing window due to rapid hardening and some delays at the initial start-up created difficulties, the material proved to be printable. Certain limits were identified as the for the 8 mm nozzle, the 2 mm aggregates in the mixture were not ideal. Overall, the 3D- printing try-out was promising, and the results indicate good potential.

6.2.4 Outlook on accelerator use in MK-GBFS based blended mixtures

The viscosity changes during the mixing procedure, the silicon pump test, calorimetric measurement as well as the results from the setting time measurement, noticeably demonstrated an accelerating effect for both HM4 and HM7, with 3% ACC. The results of the strength development of accelerated mixtures HM4 and HM7 with 3% ACC, show just minor changes, which indicates that the influence of the accelerator on strength development is limited. Literature of OPC- shotcrete based shotcrete systems show that higher dosages of ACC might lead to higher early strength, but in some cases also unwanted effects, higher greater shrinkage, higher porosity and lower durability[45], [46]. For AAMS, due to the complex formation of AAMs, similar trends were expected. High dosages of ACC or aluminosilicate could fasten the early kinetics of AAMs but might also have some

unwanted effect, heterogeneous gel networks, altered porosity or local reaction inhomogeneities. In this study, the invested MK-GBFS mixtures with 3%ACC showed accelerated early kinetics, without negatively affecting compressive strength. According to the manufacturer [30], the optimum ACC dosage is between around 3-4% ACC for shotcrete, the same amount was therefore tested. Furthermore, MK-GBFS mixtures with higher quantities of ACC 5%, 7%, were tested, for early strength development 3h-24h, hence the difference between the results were minimal and therefore no observable negative effects were visible. While higher dosages of ACC on these mixtures have not been systematically investigated, literature references from both Shotcrete OPC [45], [46] and AAM systems[44] imply that overdosing accelerators could lead to unwanted effects, highlighting the importance of dosage optimization in AAM formulations. During the silicon pump test, it was also shown that early structural build up for the HM4_3%ACC as well as HM7_3%ACC was slightly enhanced compared to the non-accelerated mixtures (HM4, HM7). Nevertheless, the printing trials showed that the non-accelerated mixtures (HM4, HM7) already exhibit a narrow workability window for printing. The role of the accelerator therefore appears less critical for enabling printability, but rather for increasing early structural build-up and improving robustness against process-related variations. In addition, a longer opening time (before setting of the mixture starts) for the developed mixtures (HM4, HM7) would be beneficial. Considering the earlier setting start of the accelerated mixtures HM4_3%ACC and HM7_3%ACC, processing might be more challenging. Moreover, to print with an ACC the laboratory requirements are higher, since a two-component printer is required which allows the addition of the ACC shortly before extrusion and layer build. With fast-reacting AAM systems such as those described in this thesis (HM4, HM7) that use a blended MK-GBFS formulations, there is only limited demand for an accelerator, whereas this could be relevant for slower AAM systems that use different precursor materials.

7 CONCLUSION

In this study, mixtures based on granulated blast furnace slag (GBFS) and metakaolin were adapted to obtain printable AAM formulations. In addition, tests were carried out to determine whether sodium-aluminate-based shotcrete accelerator can be effectively applied in alkali activated systems. The results show that the precise adjustment of chemical composition, either by variations in precursor contents or the addition of additives, are needed to achieve suitable rheological properties, strength development and reactivity in the early stages. Rheological tests showed that mixtures with excessive rheology modifier (attapulgite clay) content had lower flowability and higher thixotropy, while optimal formulations achieved a spread diameter of 115–130 mm, ensuring good workability without segregation. The addition of the accelerator had a certain impact on the setting time and overall reaction kinetics, while only showing limited effects on the mechanical properties of the materials. The results of the setting time and calorimetry tests indicate the accelerating effect of the accelerator. The significant differences in the reaction curve and setting times also showed that the addition of 3% ACC significantly improved the early reaction kinetics and polymerisation corresponding polycondensation reactions. After seven days, the developed hybrid mixtures exceeded the compressive strength range of the reference material (45–55 MPa) and reached up to 68 MPa. In pumpability and printability tests, GBFS/MK-based hybrid mixtures (HM4 and HM7) enabled stable extrusion and layer formation up to 9-11 layers, outperforming the reference mixtures, which either remained too fluid or solidified too quickly, although this could also be related to the limitations of the tests. Although the addition of the 3% ACC for both developed mixtures (HM4_3%ACC and HM7_3%ACC) indicated the enhancement of the early reaction kinetics and early strength development of the mixture, the results show that the acceleration, is not a necessity to achieve the printability of the developed mixtures (HM4, HM7). But rather, an improved earlier structural build up. Overall, the results confirm that the developed optimised AAM compositions can achieve high early strength, controlled rheology and improved printability, making them a promising more sustainable alternative to conventional cementitious materials for 3D printing. For further analysis of the material, it is crucial to determine the limits of printability and characterise the microstructure. In addition, an examination of the general composition is necessary to ensure a comprehensive understanding of the material properties.

8 REFERENCES

[1] J. Fořt, M. Mildner, M. Keppert, V. Pommer, and R. Černý, "Experimental and Environmental Analysis of High-Strength Geopolymer Based on Waste Bricks and Blast Furnace Slag," *Polymers (Basel)*, vol. 15, no. 14, Jul. 2023, doi: 10.3390/polym15143092.

[2] K. Chen, Q. Liu, B. Chen, S. Zhang, L. Ferrara, and W. Li, "Effect of raw materials on the performance of 3D printing geopolymer: A review," *Journal of Building Engineering*, vol. 84, May 2024, doi: 10.1016/j.jobe.2024.108501.

[3] Eurostat, "Waste statistics - Statistics Explained." Accessed: Nov. 04, 2025. [Online]. Available: https://ec.europa.eu/eurostat/statistics-explained/index.php?title=Waste_statistics

[4] L. Ricciotti, A. Apicella, V. Perrotta, and R. Aversa, "Geopolymer Materials for Extrusion-Based 3D-Printing: A Review," *Polymers (Basel)*, vol. 15, no. 24, Dec. 2023, doi: 10.3390/polym15244688.

[5] X. Yang *et al.*, "Effects of GBFS content and curing methods on the working performance and microstructure of ternary geopolymers based on high-content steel slag," *Constr. Build. Mater.*, vol. 410, Jan. 2024, doi: 10.1016/j.conbuildmat.2023.134128.

[6] Recyclingportal, "Euroslag-Zahlen für 2023: Eisenhüttenschlacken ersetzen 44 Millionen Tonnen Naturgestein." Accessed: Oct. 30, 2025. [Online]. Available: https://recyclingportal.eu/archive/85822

[7] C. Ziejewska *et al.*, "3D Printing of Concrete-Geopolymer Hybrids," *Materials*, vol. 15, no. 8, Apr. 2022, doi: 10.3390/ma15082819.

[8] J. L. Provis, A. Palomo, and C. Shi, "Advances in understanding alkali-activated materials," *Cem. Concr. Res.*, vol. 78, pp. 110–125, Dec. 2015, doi: 10.1016/j.cemconres.2015.04.013.

[9] M. H. Raza, R. Y. Zhong, and M. Khan, "Recent advances and productivity analysis of 3D printed geopolymers," *Addit. Manuf.*, vol. 52, pp. 21–25, Apr. 2022, doi: 10.1016/j.addma.2022.102685.

[10] C. Li, H. Sun, and L. Li, "A review: The comparison between alkali-activated slag (Si + Ca) and metakaolin (Si + Al) cements," *Cem. Concr. Res.*, vol. 40, no. 9, pp. 1341–1349, 2010, doi: 10.1016/j.cemconres.2010.03.020.

[11] P. Barve, A. Bahrami, and S. Shah, “Geopolymer 3D printing: a comprehensive review on rheological and structural performance assessment, printing process parameters, and microstructure,” *Front. Mater.*, vol. 10, 2023, doi: 10.3389/fmats.2023.1241869.

[12] P. Youssef, M. S. El-Feky, A. M. Ragab, and M. I. Serag, “Characterization of geopolymer composites for 3D printing: a microstructure approach,” *Innovative Infrastructure Solutions*, vol. 9, no. 5, May 2024, doi: 10.1007/s41062-024-01469-7.

[13] S. C. Paul, Y. W. D. Tay, B. Panda, and M. J. Tan, “Fresh and hardened properties of 3D printable cementitious materials for building and construction,” *Archives of Civil and Mechanical Engineering*, vol. 18, no. 1, pp. 311–319, Jan. 2018, doi: 10.1016/J.ACME.2017.02.008.

[14] Y. Tarhan, İ. H. Tarhan, and R. Şahin, “Comprehensive Review of Binder Matrices in 3D Printing Construction: Rheological Perspectives,” *Buildings*, vol. 15, no. 1, Jan. 2025, doi: 10.3390/buildings15010075.

[15] X. Zhou, G. Liu, Y. Bai, and H. Zhang, “Research progress on 3D printed geopolymer materials,” *Vibroengineering Procedia*, vol. 59, pp. 216–222, Sep. 2025, doi: 10.21595/vp.2025.25087.

[16] M. J. Bassan de Moraes, E. Y. Nagata, A. J. Felício Peres Duran, and J. A. Rossignolo, “Alkali activated materials applied in 3D printing construction: A review,” *Heliyon*, vol. 10, no. 5, Mar. 2024, doi: 10.1016/j.heliyon.2024.e26696.

[17] S. G. K. Mohan Kumar, J. M. Kinuthia, J. Oti, and B. O. Adeleke, “Geopolymer Chemistry and Composition: A Comprehensive Review of Synthesis, Reaction Mechanisms, and Material Properties—Oriented with Sustainable Construction,” *Materials*, vol. 18, no. 16, pp. 10–13, Aug. 2025, doi: 10.3390/ma18163823.

[18] Newchem GmbH., “Metaver ® O Metakaolin-puzzolanisch erhärtender Zusatzstoff für hydraulische Baustoffe,” Baden, Austria, 2019. [Online]. Available: www.newchem.info

[19] Newchem GmbH., “Produktinformation Metaver R,” Pfäffikon, Switzerland, 2019. Accessed: Aug. 22, 2025. [Online]. Available: http://www.newchem.info/

[20] J. Oti, B. O. Adeleke, P. R. Mudiyanselage, and J. Kinuthia, “A Comprehensive Performance Evalu0ation of GGBS-Based Geopolymer Concrete Activated by a Rice Husk Ash-Synthesised

Sodium Silicate Solution and Sodium Hydroxide," *Recycling*, vol. 9, no. 2, Apr. 2024, doi: 10.3390/recycling9020023.

[21] K. Weise, *Die Reaktivität von Hüttensand als Betonzusatzstoff: Eine thermogravimetrische Systemstudie*. Darmstadt, Deutschland: E.A.B. Koenders, Springer Vieweg, 2017. [Online]. Available: http://www.springer.com/series/15577

[22] J. Kwasny, M. Soutsos, J. A. Mcintosh, and D. J. Cleland, "banahCEM-comparison of properties of a laterite-based geopolymer with conventional concrete," 2016. [Online]. Available: http://go.qub.ac.uk/oa-feedback

[23] Y. Seyrek *et al.*, "Optimizing fiber type and content in geopolymer–oil composites: A multi-criteria performance analysis," *Constr. Build. Mater.*, vol. 489, Aug. 2025, doi: 10.1016/j.conbuildmat.2025.142218.

[24] BASF Corporation, "ATTAGEL® 40 (technical data sheet)." Accessed: Sep. 01, 2025. [Online]. Available: https://dispersions-resins-products.basf.us/products/attagel-40

[25] Sika, "Produktdatenblatt SikaControl® AER-200 P Reaktiver Luftporenbildner in Pulverform für Trockenmörtel Beschreibung," 2020. [Online]. Available: www.sika.at

[26] Austrian Standards Institute, "ÖNORM EN 1015-3: Methods of test for mortar for masonry – Part 3: Determination of consistence of fresh mortar," Vienna, 2007.

[27] C. Grengg *et al.*, "Alkali activated steel slag – oil composites: Towards resource efficiency and CO2 neutrality," *Cem. Concr. Res.*, vol. 186, Dec. 2024, doi: 10.1016/j.cemconres.2024.107678.

[28] Sika, "Sigunit® L22: Liquid accelerator for gunite & shotcrete," 2024. Accessed: Aug. 20, 2025. [Online]. Available: https://autospec.co.za/productmedia/sika/datasheets/sigunitl22.htm

[29] Y. W. D. Tay, Y. Qian, and M. J. Tan, "Printability region for 3D concrete printing using slump and slump flow test," *Compos. B Eng.*, vol. 174, Oct. 2019, doi: 10.1016/j.compositesb.2019.106968.

[30] O. Rudić *et al.*, "On the benefits of vegetable oil addition for the pore structure and acid resistance of alkali-activated systems," *Ceram. Int.*, vol. 49, no. 20, pp. 33275–33290, Oct. 2023, doi: 10.1016/j.ceramint.2023.08.036.

[31] F. R. Steindl *et al.*, “Innovative upcycling approaches for slags and mineral wastes: Transforming secondary raw materials into novel building materials,” in *International Slag Valorisation Symposium* , Apr. 2025, pp. 243–245.

[32] Austrian Standards International, “ÖNORM EN 196-3:2016 – Prüfverfahren für Zement – Teil 3: Bestimmung der Erstarrungszeit und der Raumbeständigkeit,” Vienna, 2016.

[33] Austrian Standards International, “DIN EN 1015-11:2020-01 - Methods of test for mortar for masonry – Part 11: Determination of flexural and compressive strength of hardened mortar,” Vienna, 2020.

[34] MAI International GmbH., “MAI® 2PUMP PICTOR-3D: Technische Daten für 3D-Betondruck Produktdatenblatt,” Jan. 2025. [Online]. Available: https://mai.at/de/produktgruppen/3d-betondruck/mai-2pump-pictor-3d/

[35] WASP – World’s Advanced Saving Project S.p.A. (n.d.)., “WASP 40100 LDM Technical specifications.” Accessed: Jan. 31, 2026. [Online]. Available: https://3dwasp.com/en/ceramic-3d-printer-wasp-40100-ldm/

[36] J. Jauk, H. Vašatko, L. Gosch, I. Christian, A. Klaus, and M. Stavric, “Digital fabrication of growth:Combining digital manufacturing of clay with natural growth of mycelium,” in *26th International Conference of the Association for Computer-Aided Architectural Design Research* , Caaderia, Asia, 2021, pp. 753–762.

[37] H. Di, “Application Analysis of Colloidal Attapulgite Clay in Refractory Materials,” Active Minerals International LLC, 2023.

[38] Hermann Di, Jeason Fan, and Ningsheng Zhou, “Application analysis of colloidal attapulgite clay in refractory materials.” [Online]. Available: https://activeminerals.com/blog/application-analysis-of-colloidal-attapulgite-clay-in-refractory-materials/

[39] E. Najafi Kani, A. Allahverdi, and J. L. Provis, “Calorimetric study of geopolymer binders based on natural pozzolan,” *J. Therm. Anal. Calorim.*, vol. 127, no. 3, pp. 2181–2190, Mar. 2017, doi: 10.1007/s10973-016-5850-7.

[40] A. Usherov-marshak, D. Vaičiukynienė, P. Krivenko, and G. Bumanis, “Calorimetric studies of alkali-activated blast-furnace slag cements at early hydration processes in the temperature range of 20–80 °C,” *Materials*, vol. 14, no. 19, Oct. 2021, doi: 10.3390/ma14195872.

[41] H. Kruppa, M. Kalthoff, A. Vollpracht, and T. Matschei, “Entwicklung eines alkalisch aktivierten Bindemittels für das Extrusionsverfahren,” *ce/papers*, vol. 6, no. 6, pp. 783–789, Dec. 2023, doi: 10.1002/cepa.2825.

[42] J. L. Provis and J. S. J. Van Deventer, *Alkali Activated Materials: RILEM State-of-the-Art Reports*, vol. 13. doi: 10.1007/978-94-007-7672-2.

[43] J. Wang *et al.*, “Effect of accelerator dosage on the moisture transfer properties of shotcrete: From the perspective of pore structures,” *Constr. Build. Mater.*, vol. 493, Sep. 2025, doi: 10.1016/j.conbuildmat.2025.143113.

[44] M. J. Garba *et al.*, “Effect of accelerators on the long-term performance of shotcrete and its improvement strategies: A review,” Jul. 15, 2024, *Elsevier Ltd*. doi: 10.1016/j.jobe.2024.109364.

9 LIST OF FIGURES

10 LIST OF GRAPHICAL ABSTRACTS

11 LIST OF TABLES

Appendix

Calorimeter

The exact weight of the ingredients (Table 12) the exact time when the waterglass (WG) or accelerator (ACC) was added were noted for the calorimeter measurement and is visible below in Table 13.

Table 12 Indeed and ideal weight in [g] of the samples for the IC calorimeter measurement

Mixture	Amount of ACC	weight	HÜS [g]	MO [g]	MR [g]	Ae [g]	Atag [g]	UBF [g]	H_2O [g]	Oil [g]	WG 1.7 [g]	L22 [g]	Fluid sum [g]	Sum solids [g]
HM4	0%	Ideal	179.8	59.9	0	0.6	5.9	0	6.7	19.2	143.8	0	90.55	325.29
		Indeed	179.81	59.9	0	0.6	5.91	0	6.71	19.21	143.86	0	90.66	325.34
	3%	Ideal	179.8	59.9	0	0.6	5.9	0	6.7	19.2	143.8	7.5	94.8	325.29
		Indeed	179.84	59.94	0	0.6	5.95	0	6.71	19.22	143.82	7.55	94.95	325.43
HM7	0%	Ideal	167.6	29.1	29.1	0.5	4.6	0	0	23.1	157	0	93.76	317.24
		Indeed	167.6	29.12	29.13	0.49	4.6	0	0	23.14	157.3	0	93.93	317.46
	3%	Ideal	167.6	29.1	29.1	0.5	4.6	0	0	23.1	157	7	97.76	317.24
		Indeed	167.57	29.08	29.07	0.47	4.6	0	0	23.13	157.02	7.19	97.89	317.15

Table 13 Noted time for the addition of WG or ACC

Mixture	Amount of ACC	Date	Test start / addition of WG	Addition of ACC	Mass start [g]	Mass 50g label
HM4	0%	02.04.2025	13:04	-	50.57	50g
	3%	02.04.2025	14:01	14:07	49.95	50g
HM7	0%	02.04.2025	14:35	-	49.97	50g
	3%	02.04.2025	15:12	15:17	50.34	50g